Electronic Supporting Information

Synthesis and Living Crystallization-Driven Self-Assembly of Backbone Asymmetric and Symmetric π-Conjugated Oligo(*p*-phenylene ethynylene)-Based Block Copolymers

Jiucheng Nie,[a,c] *Xiaoyu Huang*,[a,c,*] *Guolin Lu*,[a] *Mitchell A. Winnik*,[d,e,*] *Chun Feng*[a,b,*]

[a] Key Laboratory of Synthetic and Self-Assembly Chemistry for Organic Functional Molecules, Center for Excellence in Molecular Synthesis, Shanghai Institute of Organic Chemistry, University of Chinese Academy of Sciences, Chinese Academy of Sciences, 345 Lingling Road, Shanghai 200032, People's Republic of China

[b] Shanghai Key Laboratory of Advanced Polymeric Materials, School of Materials Science and Engineering, East China University of Science and Technology, 130 Meilong Road, Shanghai 200237, People's Republic of China

[c] School of Physical Science & Technology, ShanghaiTech University, 100 Haike Road, Shanghai 201210, People's Republic of China

[d] Department of Chemistry, University of Toronto, 80 St. George St, Toronto, Ontario M5S 3H6, Canada

[e] Department of Chemical Engineering and Applied Chemistry, University of Toronto, Toronto, ON M5S 3E2

* To whom correspondence should be addressed, E-mail: cfeng@mail.sioc.ac.cn (Tel: +86-21-54925606, Fax: +86-21-64166128), m.winnik@utoronto.ca (Tel: +1-416-978-6495), xyhuang@mail.sioc.ac.cn (Tel: +86-21-54925310, Fax: +86-21- 64166128).

SUPPORTING EXPERIMENTAL DETAILS

Materials

Ethanol (≥99.8%, Aladdin) and tetrahydrofuran (THF, 99.9%, Aladdin) were used as received without further purification. Other reagents not specially mentioned were purchased from Aladdin and used as received without further purification. Monomers of **1c**, **1g, 1i** and oligomers of **2g**, **5b**, **7b** were the same samples in our previous report.[1] $PNIPAM_{22}$ and OPE-based block copolymers were synthesized and purified in a similar way as described in our previous report.[1]

Instrumentation

^1H NMR (400 MHz) analyses were performed on a JEOL JNM-ECZ400 spectrometer in $CDCl_3$ or CD_2Cl_2, tetramethylsilane (TMS) was used as internal standard. Relative molecular weights and molecular weight distributions were measured by conventional size exclusion chromatography (SEC) using a system equipped with a Waters 1515 Isocratic HPLC pump, a Waters 2414 refractive index detector, a Waters 2487 dual λ absorbance detector and a set of Waters Styragel columns (HR3 (500-30,000), HR4 (5,000-600,000) and HR5 (50,000-4,000,000), 7.8×300 mm, particle size: 5 μm). SEC measurements were carried out at 35°C using THF as eluent with a flow rate of 1.0 mL/min. The system was calibrated with linear polystyrene standards.

Matrix-assisted laser desorption/ionization time of flight mass spectrometry (MALDI-TOF)

Small aliquots of sample solution (2 μL, 1.0 mg/mL) in CH_2Cl_2 were added to a sample plate for MALDI-TOF measurement. After drying in air at room temperature (~10 min), an aliquot of α-cyano-4-hydroxy cinnamic acid (2 μL, 5.0 mg/mL) dispersed in an acetonitrile/water mixture (v/v = 1/1) was added and allowed to dry in air at room temperature. MALDI-TOF spectra were obtained on a Waters MICROMASS MALDI micro MX mass spectrometer.

Transmission electron microscopy (TEM)

TEM images were obtained by a JEOL JEM-2100 instrument operated at 80 kV. A drop of micellar solution (10 μL) was placed on a Formvar and carbon-coated copper grid for 10 s and then a filter paper touched the edge of drop to absorb most of liquid on the grid. The grid was allowed to dry at room temperature. For the samples stained by phosphotungstic acid, after the grid was dried (*ca*. 10 s after touching with filter paper), a drop of phosphotungstic acid aqueous solution (10 μL, 1.0 mg/mL) was placed onto the surface. After 10 s, most of the solution on the grid was absorbed by touching the edge of the drop with a filter paper, and then the grid was allowed to dry at room temperature. For each sample, the length distribution of micelles was determined by tracing more than 100 individual micelles, and width distributions were determined by making measurements at least 100 different positions on several micelles and analysis using the ImageJ software program from National Institutes of Health. Values of number-average length (L_n), weight-average length (L_w), number- average width (W_n) and weight-average width (W_w) of micelles were calculated as follows:

$$L_n = \frac{\sum_{i=1}^{N} N_i L_i}{\sum_{i=1}^{N} N_i} \quad (1)$$

$$L_w = \frac{\sum_{i=1}^{N} N_i L_i^2}{\sum_{i}^{N} N_i L_i} \quad (2)$$

$$W_n = \frac{\sum_{i=1}^{N} N_i W_i}{\sum_{i=1}^{N} N_i} \quad (3)$$

$$W_w = \frac{\sum_{i}^{N} N_i W_i^2}{\sum_{i=1}^{N} N_i W_i} \quad (4)$$

where N_i is the number of micelles of length L_i or width W_i, and N is the number of calculated micelles in each sample. The distribution of micellar length or width is characterized by both L_w/L_n or W_n/W_i and the standard deviation of the length distribution σ.

Atomic force microscopy (AFM)

AFM images were acquired in air in tapping mode using a JPK NanoWizard Sense system. Aliquots (10 μL) of micellar solution prepared as described were deposited on mica and dried at room temperature in air.

UV/vis and fluorescence spectroscopy

UV/vis absorption spectra were recorded on a Hitachi U-2910 spectrophotometer. Fluorescence emission spectra were measured by using a Hitachi F-2700 fluorescence spectrophotometer with a 5 nm band width. Convenient UV/vis and fluorescence measurements were performed at room temperature.

Polydisperse fiber-like micelles were first obtained by heating the solutions of D-OPE$_7$-*b*-PNIPAM$_{22}$ (ethanol/water, v/v = 75/25, 0.2 mg/mL), S-OPE$_7$-*b*-PNIPAM$_{22}$ (ethanol/water, v/v

= 90/10, 0.2 mg/mL), D-OPE_8-*b*-$PNIPAM_{22}$ (ethanol, 0.2 mg/mL) and S-OPE_8-*b*- $PNIPAM_{22}$ (ethanol, 0.2 mg/mL) at 80°C for 30 min, followed by cooling in air and aging at room temperature (23°C) for 24 h (heating/cooling process). Subsequently, corresponding seed micelles were obtained by mild sonication at 0°C for 30 min. Suspensions of seed micelles with varying concentrations (0.01, 0.02, 0.05 and 0.10 mg/mL) were prepared by dilution from corresponding mother seed solution with concentration of 0.2 mg/mL.

For the temperature-dependent UV/vis absorption measurements, the temperature of the cell housing (1 cm path cell) was controlled with a Neslab RTE-110 bath. Temperature-dependent UV/vis measurements were conducted by heating the samples (solutions of seed micelles with different concentrations) from 23°C with a rate of 0.5°C/min. After the solutions were maintained at each target temperature for 5 min, UV/vis absorption spectra were recorded.

X-ray diffraction (XRD) analysis

XRD measurements were conducted by Philips X'Pert PRO X-ray powder diffractometer with Cu*Kα* (1.541 Å) radiation (40 kV, 40 mA) and samples were exposed at a scan rate of 2θ = 0.0334°/s between 3° and 30°. Alkyne-terminated OPE_n samples were prepared by casting CH_2Cl_2 solution of OPE_n onto a silicon wafer, and allowing them to dry at room temperature, respectively.

Oligomer and Polymer Syntheses

Syntheses of OPE_n

All alkyne-terminated OPE_n samples were synthesized and purified in a similar way (**Scheme S1**) as described in our previous report.[1]

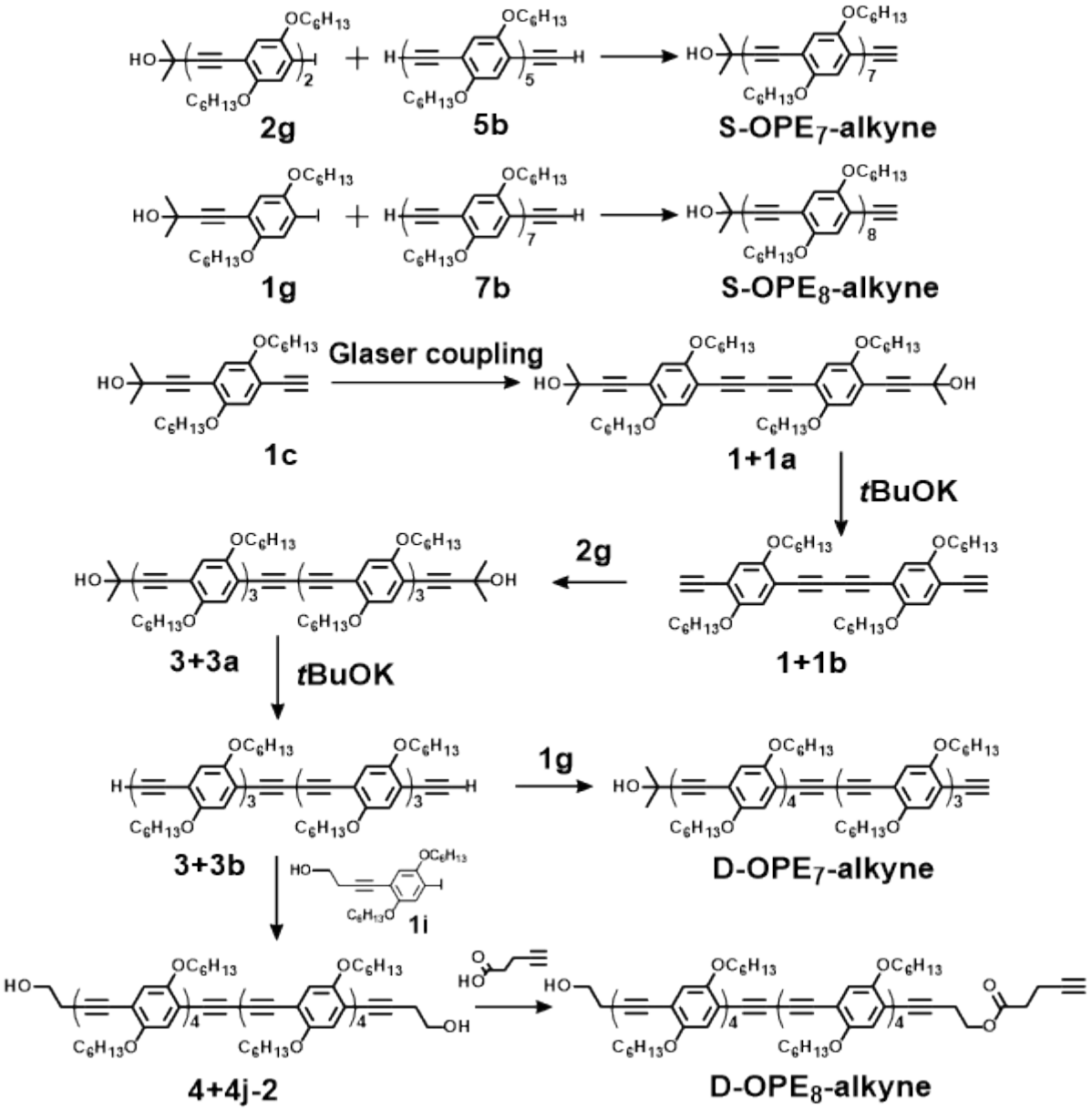

Scheme S1. Synthetic route of alkyne-terminated OPE_n.

Synthesis of S-OPE$_7$-alkyne

5b (200 mg, 0.13 mmol), **2g** (100 mg, 0.13 mmol), [$Pd(PPh_3)_2Cl_2$] (3 mg, 0.004 mmol) and CuI (1 mg, 0.005 mmol) were added into a 10 mL Schlenk flask, followed by degassing and kept under N_2. Next, THF (2.5 mL) and TEA (2.5 mL) were added via a gastight syringe followed by stirring at room temperature for 5 h. The solvent was evaporated *in vacuo* and the crude product was purified by silica column chromatography (eluent: CH_2Cl_2/petroleum ether = 4/1) to give **S-OPE$_7$-alkyne** (62 mg, 22%) as a yellow solid. The product was subjected to MALDI-TOF (**Figure 1A**), SEC (**Figure 1B**) and ^{1}H NMR (**Figure 1C**). MALDI-TOF: calculated $C_{145}H_{204}O_{15}$ for 2187.21; found 2187.0 [M+]. SEC: M_n^{SEC} = 3800 g/mol, M_w/M_n = 1.01. ^{1}H NMR (400 MHz, $CDCl_3$): δ (ppm): 0.87 (m, 42H, $OCH_2CH_2(CH_2)_3CH_3$), 1.33-1.51 (m, 84H, $OCH_2CH_2(CH_2)_3CH_3$), 1.63 (s, 6H, $C(CH_3)_2OH$), 1.84 (m, 28H, $OCH_2CH_2(CH_2)_3CH_3$), 3.34 (s, 1H, alkyne *H*), 4.02 (m, 28H, $OCH_2CH_2(CH_2)_3CH_3$), 6.89-7.00 (m, 14H, Ar*H*).

Synthesis of S-OPE$_8$-alkyne

7b (200 mg, 0.094 mmol), **1g** (46 mg, 0.094 mmol), [$Pd(PPh_3)_2Cl_2$] (7 mg, 0.009 mmol) and CuI (2 mg, 0.009 mmol) were added into a 10 mL Schlenk flask, followed by degassing and kept under N_2. Next, THF (3 mL) and TEA (3 mL) were added via a gastight syringe followed by stirring at room temperature for 5 h. The solvent was evaporated *in vacuo* and the crude product was purified by silica column chromatography (eluent: CH_2Cl_2/ethyl acetate = 100/1) to give **S-OPE$_8$-alkyne** (50 mg, 21%) as a yellow solid. The product was subjected to MALDI-TOF (**Figure 1A**), SEC (**Figure 1B**) and ^{1}H NMR (**Figure 1C**). MALDI-TOF: calculated

$C_{165}H_{232}O_{17}$ for 2487.65; found 2487.3 [M+]. SEC: M_n^{SEC} = 4000 g/mol, M_w/M_n = 1.01. ^{1}H NMR (400 MHz, $CDCl_3$): δ (ppm): 0.88 (m, 48H, $OCH_2CH_2(CH_2)_3CH_3$), 1.33-1.51 (m, 96H, $OCH_2CH_2(CH_2)_3CH_3$), 1.63 (s, 6H, $C(CH_3)_2OH$), 1.84 (m, 32H, $OCH_2CH_2(CH_2)_3CH_3$), 3.33 (s, 1H, alkyne *H*), 4.02 (m, 32H, $OCH_2CH_2(CH_2)_3CH_3$), 6.90-7.01 (m, 16H, Ar*H*).

Synthesis of 1+1a

1c (3.61 g, 9.39 mmol), $[Pd(PPh_3)_2Cl_2]$ (108 mg, 0.154 mmol) and CuI (90 mg, 0.47 mmol) were added into a 100 mL flask. Next, THF (20 mL) and TEA (20 mL) were added followed by stirring at room temperature overnight. The solvent was evaporated *in vacuo* and the crude product was purified by silica column chromatography (eluent: CH_2Cl_2/ethyl acetate = 30:1) to give **1+1a** as a pale yellow solid (3.54 g, 98%). MALDI-TOF: calculated $C_{50}H_{70}O_6$ for 767.10; found 766.5 [M+]. ^{1}H NMR (400 MHz, $CDCl_3$): δ (ppm): 0.89 (m, 12H, $OCH_2CH_2(CH_2)_3CH_3$), 1.33-1.48 (m, 24H, $OCH_2CH_2(CH_2)_3CH_3$), 1.61 (s, 12H, $C(CH_3)_2OH$), 1.77 (m, 8H, $OCH_2CH_2(CH_2)_3CH_3$), 3.95 (m, 8H, $OCH_2CH_2(CH_2)_3CH_3$), 6.86 (s, 2H, Ar*H*), 6.92 (s, 2H, Ar*H*).

Synthesis of 1+1b

1+1a (1.8 g, 2.35 mmol) and potassium *tert*-butoxide (*t*BuOK, 0.21 g, 1.88 mmol) were added into a 100 mL flask containing 60 mL of toluene, followed by stirring at 95 ℃ for 10 min. The solvent was evaporated *in vacuo* and the crude product was purified by silica column chromatography (eluent: CH_2Cl_2/petroleum ether = 2/1) to give **1+1b** as a pale yellow solid (1.46 g, 95%). ^{1}H NMR (400 MHz, $CDCl_3$): δ (ppm): 0.89 (m, 12H, $OCH_2CH_2(CH_2)_3CH_3$),

1.33-1.47 (m, 24H, $OCH_2CH_2(CH_2)_3CH_3$), 1.79 (m, 8H, $OCH_2CH_2(CH_2)_3CH_3$), 3.35 (s, 2H, alkyne *H*), 3.96 (m, 8H, $OCH_2CH_2(CH_2)_3CH_3$), 6.94 (s, 2H, Ar*H*), 6.95 (s, 2H, Ar*H*).

Synthesis of 3+3a

1+1b (500 mg, 0.768 mmol), **2g** (725 mg, 0.922 mmol), $[Pd(PPh_3)_2Cl_2]$ (28 mg, 0.039 mmol) and CuI (8 mg, 0.039 mmol) were added into a 100 mL Schlenk flask, followed by degassing and kept under N_2. Next, THF (30 mL) and TEA (30 mL) were added via a gastight syringe followed by stirring at room temperature overnight. The solvent was evaporated *in vacuo* and the crude product was purified by silica column chromatography (eluent: CH_2Cl_2/ethyl acetate = 50:1) to give **3+3a** as a yellow solid (840 mg, 56%). ^{1}H NMR (400 MHz, $CDCl_3$): 0.87 (m, 36H, $OCH_2CH_2(CH_2)_3CH_3$), 1.33-1.50 (m, 72H, $OCH_2CH_2(CH_2)_3CH_3$), 1.63 (s, 12H, $C(CH_3)_2OH$), 1.83 (m, 24H, $OCH_2CH_2(CH_2)_3CH_3$), 4.01 (m, 24H, $OCH_2CH_2(CH_2)_3CH_3$), 6.89-6.99 (m, 12H, Ar*H*).

Synthesis of 3+3b

3+3a (750 mg, 0.38 mmol) and *t*BuOK (120 mg, 1.07 mmol) were added to 50 mL of toluene, followed by stirring at 110 °C for 30 min. After filtration of solution and evaporation of solvent, the crude product was purified by silica column chromatography (eluent: CH_2Cl_2/petroleum ether = 2/3) to give **3+3b** as a yellow solid (300 mg, 42%). MALDI-TOF: calculated $C_{124}H_{170}O_{12}$ for 1852.71; found 1852.6 [M+]. ^{1}H NMR (400 MHz, $CDCl_3$): δ (ppm): 0.87 (m, 36H, $OCH_2CH_2(CH_2)_3CH_3$), 1.33-1.50 (m, 72H, $OCH_2CH_2(CH_2)_3CH_3$), 1.82 (m, 24H,

$OCH_2CH_2(CH_2)_3CH_3$), 3.33 (s, 2H, alkyne *H*), 4.00 (m, 24H, $OCH_2CH_2(CH_2)_3CH_3$), 6.96-6.99 (m, 12H, Ar*H*).

Synthesis of D-OPE$_7$-alkyne

3+3b (200 mg, 0.108 mmol), **1g** (53 mg, 0.108 mmol), $[Pd(PPh_3)_2Cl_2]$ (2 mg, 0.003 mmol) and CuI (1 mg, 0.004 mmol) were added into a 10 mL Schlenk flask, followed by degassing and kept under N_2. Next, THF (3 mL) and TEA (3 mL) were added via a gastight syringe followed by stirring at room temperature for 5 h. The solvent was evaporated *in vacuo* and the crude product was purified by silica column chromatography (eluent: CH_2Cl_2/petroleum ether = 4/1) to give **D-OPE$_7$-alkyne** (57 mg, 24%) as a yellow solid. The product was subjected to MALDI-TOF (**Figure 1A**), SEC (**Figure 1B**) and ^{1}H NMR (**Figure 1C**). MALDI-TOF: calculated $C_{147}H_{204}O_{15}$ for 2211.23; found 2211.5 [M+]. SEC: M_n^{SEC} = 3400 g/mol, M_w/M_n = 1.01. ^{1}H NMR (400 MHz, $CDCl_3$): δ (ppm): 0.87 (m, 42H, $OCH_2CH_2(CH_2)_3CH_3$), 1.33-1.50 (m, 84H, $OCH_2CH_2(CH_2)_3CH_3$), 1.63 (s, 6H, $C(CH_3)_2OH$), 1.82 (m, 28H, $OCH_2CH_2(CH_2)_3CH_3$), 3.33 (s, 1H, alkyne *H*), 4.01 (m, 28H, $OCH_2CH_2(CH_2)_3CH_3$), 6.96-6.99 (m, 14H, Ar*H*).

Synthesis of 4+4j-2

3+3b (225 mg, 0.121 mmol), **1i** (132 mg, 0.279 mmol), $[Pd(PPh_3)_2Cl_2]$ (4 mg, 0.006 mmol) and CuI (1 mg, 0.004 mmol) were added into a 50 mL Schlenk flask, followed by degassing and kept under N_2. Next, THF (10 mL) and TEA (10 mL) were added via a gastight syringe followed by stirring at room temperature overnight. The solvent was evaporated *in vacuo* and the crude product was purified by silica column chromatography (eluent: CH_2Cl_2/ethyl acetate

= 50:1) to give **4+4j-2** as a yellow solid (120 mg, 40%). MALDI-TOF: calculated $C_{168}H_{234}O_{18}$ for 2541.70; found 2541.0 [M+]. ^{1}H NMR (400 MHz, $CDCl_3$): δ (ppm): δ (ppm): 0.87 (m, 48H, $OCH_2CH_2(CH_2)_3CH_3$), 1.33-1.51 (m, 96H, $OCH_2CH_2(CH_2)_3CH_3$), 1.84 (m, 32H, $OCH_2CH_2(CH_2)_3CH_3$), 2.73 (t, J = 6.04 Hz, 4H, CH_2CH_2OH), 3.81 (t, J = 5.99 Hz, 4H, CH_2CH_2OH), 4.02 (m, 32H, $OCH_2CH_2(CH_2)_3CH_3$), 6.89-6.99 (m, 16H, Ar*H*).

Synthesis of D-OPE$_8$-alkyne

4+4j-2 (60 mg, 0.024 mmol), *N*,*N*'-dicyclohexylcarbodiimide (DCC, 7 mg, 0.036 mmol), 4-pentynoic acid (2.3 mg, 0.024 mmol) and 4-dimethylaminopyridine (DMAP, 1 mg, 0.008 mmol) were added into a 50 mL flask containing 20 mL of dry CH_2Cl_2, followed by stirring at room temperature overnight. The solvent was evaporated *in vacuo* and the crude product was purified by silica column chromatography (eluent: CH_2Cl_2) to give **D-OPE$_8$-alkyne** as a yellow solid (15 mg, 24%). The product was subjected to MALDI-TOF (**Figure 1A**), SEC (**Figure 1B**) and ^{1}H NMR (**Figure 1C**). MALDI-TOF: calculated $C_{173}H_{238}O_{19}$ for 2621.79; found 2621.5 [M+]. SEC: M_n^{SEC} = 4200 g/mol, M_w/M_n = 1.01. ^{1}H NMR (400 MHz, $CDCl_3$): δ (ppm): 0.88 (m, 48H, $OCH_2CH_2(CH_2)_3CH_3$), 1.33-1.50 (m, 96H, $OCH_2CH_2(CH_2)_3CH_3$), 1.84 (m, 32H, $OCH_2CH_2(CH_2)_3CH_3$), 1.97 (m, 1H, alkyne *H*), 2.51 (m, 2H, $CH_2CH_2CO_2$), 2.59 (m, 2H, $CH_2CH_2CO_2$), 2.73 (t, J = 6.08 Hz, 2H, CH_2CH_2OH), 2.81 (t, J = 6.97 Hz, 2H, $CO_2CH_2CH_2$), 3.81 (t, J = 5.99 Hz, 2H, CH_2CH_2OH), 4.02 (m, 32H, $OCH_2CH_2(CH_2)_3CH_3$), 4.30 (t, J = 6.96 Hz, 2H, $CO_2CH_2CH_2$), 6.89-6.99 (m, 16H, Ar*H*).

Synthesis of OPE-*b*-PNIPAM$_{22}$ diblock copolymer

OPE-*b*-PNIPAM$_{22}$ diblock copolymers were synthesized (**Scheme S2**) and purified in a similar

way as described in our previous report.[1] Cu-catalyzed alkyne azide cycloaddition (CuAAC) reaction was used to synthesize OPE-*b*-PNIPAM$_{22}$ diblock copolymers between alkyne-terminated OPE and azide-terminated PNIPAM$_{22}$.

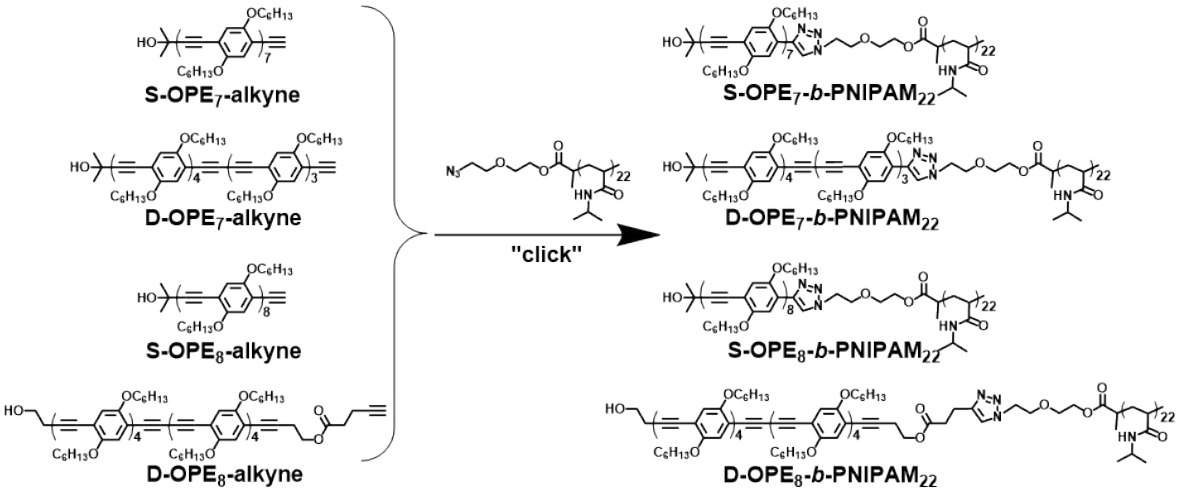

Scheme S2. Synthetic route of OPE-based BCPs.

Taking S-OPE$_7$-*b*-PNIPAM$_{22}$ as an example, S-OPE$_7$-alkyne (25 mg, 11.4 μmol), PNIPAM$_{22}$ (80 mg, 29.6 μmol), CuCl (3 mg, 30.3 μmol) and TBTA (17 mg, 32.1 μmol) were added into a 25 mL Schlenk flask followed by adding 5 mL of dry THF via a gastight syringe. The flask was degassed by three freeze-pump-thaw cycles followed by immersing the flask into an oil bath set at 50°C. The reaction mixture was allowed to stir for 24 h. The solvent was evaporated and the residue was purified by silica column chromatography (eluent: CH_2Cl_2/ ethyl acetate = 10/1) to remove the unreacted S-OPE$_7$-alkyne. To remove excess PNIPAM$_{22}$, the crude product was purified by repeated dissolution in THF and precipitation in water/ ethanol (v/v = 1/1) three times, followed by drying *in vacuo* overnight to give 42 mg (75%) of S-OPE$_7$-*b*-PNIPAM$_{22}$ diblock copolymer as yellow solid.

These diblock copolymers were subjected to SEC (**Figure S1A**) and ^{1}H NMR (**Figure S1B**), and the number-average degree of polymerization of PNIPAM block ($N_{NIPAM} = S_{a,k,p}/(S_u/42)$-

30 = 22) was determined by ^{1}H NMR on the basis of known DP_n of S-OPE$_7$-alkyne. S-OPE$_7$-*b*-PNIPAM$_{22}$, SEC: M_n^{SEC} = 7300 g/mol, M_w/M_n = 1.06.

D-OPE$_7$-*b*-PNIPAM$_{22}$, SEC: M_n^{SEC} = 7200 g/mol, M_w/M_n = 1.06.

D-OPE$_8$-*b*-PNIPAM$_{22}$, SEC: M_n^{SEC} = 8100 g/mol, M_w/M_n = 1.06.

S-OPE$_8$-*b*-PNIPAM$_{22}$, SEC: M_n^{SEC} = 7400 g/mol, M_w/M_n = 1.08.

Self-assembly Experiments

Self-assembly of S-OPE$_7$-*b*-PNIPAM$_{22}$ diblock copolymer

A concentrated THF solution (10 mg/mL) of S-OPE$_7$-*b*-PNIPAM$_{22}$ was added into hot (80^{o}C) ethanol/water (90/10, v/v) until the concentration reached 0.2 mg/mL. Subsequently, the solution was heated at 80^{o}C for 30 min, followed by cooling in air and aging at room temperature (23^{o}C) for 24 h. A drop of the resulting solution was placed on a Formvar and carbon-coated copper grid and examined by TEM (**Figure 2A**).

Self-assembly of D-OPE$_7$-*b*-PNIPAM$_{22}$ diblock copolymer

A concentrated THF solution (10 mg/mL) of S-OPE$_7$-*b*-PNIPAM$_{22}$ was added into hot (80^{o}C) ethanol/water (75/25or 90/10, v/v) until the concentration reached 0.2 mg/mL. Subsequently, the solution was heated at 80^{o}C for 30 min, followed by cooling in air and aging at room temperature (23^{o}C) for 24 h. A drop of the resulting solution was placed on a Formvar and carbon-coated copper grid and examined by TEM (**Figure 2B**). Ethanol/water (90/10, v/v) was used in contrast experiments.

Self-assembly of D-OPE$_8$-*b*-PNIPAM$_{22}$ diblock copolymer

A concentrated THF solution (10 mg/mL) of D-OPE$_8$-*b*-PNIPAM$_{22}$ was added into hot (80^{o}C) ethanol until the concentration reached 0.2 mg/mL. Subsequently, the solution was heated at 80^{o}C for 30 min, followed by cooling in air and aging at room temperature (23^{o}C) for 24 h. A drop of the resulting solution was placed on a Formvar and carbon-coated copper grid and examined by TEM (**Figure S10A**).

Self-assembly of S-OPE$_8$-*b*-PNIPAM$_{22}$ diblock copolymer

A concentrated THF solution (10 mg/mL) of S-OPE$_8$-*b*-PNIPAM$_{22}$ was added into hot (80^{o}C) ethanol until the concentration reached 0.2 mg/mL. Subsequently, the solution was heated at 80^{o}C for 30 min, followed by cooling in air and aging at room temperature (23^{o}C) for 24 h. A drop of the resulting solution was placed on a Formvar and carbon-coated copper grid and examined by TEM (**Figure S10C**).

Preparation of seed micelles

Seed micelles were prepared by sonicating (SONICS VC 750 ultrasonic processor, 30% power) the corresponding polydisperse micelles of OPE-*b*-PNIPAM$_{22}$ (0.2 mg/mL) at 0^{o}C for 30 min. A drop of fresh seed solution or seed solution after aging at room temperature (23^{o}C) for 24 h was placed on a Formvar and carbon-coated copper grid and examined by TEM (**Figures 3A**, **4A**, **S5**, **S10B & D**).

Self-seeding of S-OPE$_7$-*b*-PNIPAM$_{22}$

Self-seeding of seed micelles of S-OPE$_7$-*b*-PNIPAM$_{22}$ was conducted by thermal annealing at

different temperatures and at different concentrations. Samples with lower concentrations were diluted by ethanol/water (90/10, v/v) from the seed micelles of S-OPE$_7$-*b*-PNIPAM$_{22}$ with concentration of 0.2 mg/mL. Aliquots of seed micellar solution in several vials (0.4 mL/vial) were put into water-baths set at different temperatures and heated for 0.5 h, followed by cooling in air and aging at room temperature (23℃) for 24 h. Finally, a drop of each solution was placed on a Formvar and carbon-coated copper grid and examined by TEM (**Figures 3** & **S6**). Characterization details are summarized in **Table S1**.

Self-seeding of D-OPE$_7$-*b*-PNIPAM$_{22}$

Self-seeding of seed micelles of D-OPE$_7$-*b*-PNIPAM$_{22}$ was conducted by thermal annealing at different temperatures and at different concentrations. Samples with lower concentrations were diluted by ethanol/water (75/25, v/v) from the seed micelles of D-OPE$_7$-*b*-PNIPAM$_{22}$ with concentration of 0.2 mg/mL. Aliquots of seed micellar solution in several vials (0.4 mL/vial) were put into water-baths set with different temperatures and heated for 0.5 h, followed by cooling with water-bath in air for 24 h. Finally, a drop of each solution was placed on a Formvar and carbon-coated copper grid and examined by TEM (**Figures 4** & **S9**). Characterization details are summarized in **Table S4**.

Control experiments included using ethanol/water (75/25, v/v) or ethanol/water (90/10, v/v) as solvent. Aliquots of seed micellar solution in several vials (0.4 mL/vial) were put into water-baths set with different temperatures and heated for 0.5 h, followed by cooling in air and aging at room temperature (23℃) for 24 h. Characterization details are summarized in **Figures S7-8** and **Tables S2-3**.

Self-seeding of D-OPE$_8$-*b*-PNIPAM$_{22}$

Self-seeding of seed micelles of D-OPE$_8$-*b*-PNIPAM$_{22}$ was conducted by thermal annealing at different temperatures with different concentrations. Samples with lower concentrations were diluted by ethanol from the seed micelles of D-OPE$_8$-*b*-PNIPAM$_{22}$ with concentration of 0.2 mg/mL. Aliquots of seed micellar solution in several vials (0.4 mL/vial) were put into water-baths set with different temperatures and heated for 0.5 h, followed by immersing the vials in the water-bath set at 35℃ for 24 h. Finally, a drop of each solution was placed on a Formvar and carbon-coated copper grid and examined by TEM (**Figures 5A-B** & **S11**). Characterization details are summarized in **Table S5**.

Self-seeding of S-OPE$_8$-*b*-PNIPAM$_{22}$

Self-seeding of seed micelles of S-OPE$_8$-*b*-PNIPAM$_{22}$ was conducted by thermal annealing at different temperatures with different concentrations. Samples with lower concentrations were diluted by ethanol from the seed micelles of S-OPE$_8$-*b*-PNIPAM$_{22}$ with concentration of 0.2 mg/mL. Aliquots of seed micellar solution in several vials (0.4 mL/vial) were put into water-baths set with different temperatures and heated for 0.5 h, followed by cooling in air and aging at room temperature (23℃) for 24 h. Finally, a drop of each solution was placed on a Formvar and carbon-coated copper grid and examined by TEM (**Figures 5D-E** & **S12**). Characterization details are summarized in **Table S6**.

Preparation of seed micelles of S-OPE$_9$-*b*-P2VP$_{56}$ for seeded growth

Seed micelles of S-OPE$_9$-*b*-P2VP$_{56}$ for "heating/cooling" seeded growth were prepared according to our previous report.[1] Fresh seed micelles of S-OPE$_9$-*b*-P2VP$_{56}$ were prepared by

sonicating (SONICS VC 750 ultrasonic processor, 30% power) the corresponding polydisperse fiber-like micelles of S-OPE$_9$-*b*-P2VP$_{56}$ in ethanol (0.1 mg/mL) at 0^{o}C for 30 min. The fresh seed micelles were then annealed at 74^{o}C for 1 h and allowed to cool and age at room temperature (23^{o}C).

Preparation of ^{M}(D-OPE$_7$-*b*-PNIPAM$_{22}$)-*b*-^{M}(S-OPE$_9$-*b*-P2VP$_{56}$)-*b*-^{M}(D-OPE$_7$-*b*-PNIPAM$_{22}$) A-B-A triblock comicelles by seeded growth approach

Aliquots (1 and 3 μL) of a concentrated THF solution of D-OPE$_7$-*b*-PNIPAM$_{22}$ (2.5 mg/mL) were added into 475 μL of hot ethanol/water (70℃, 415 μL/60 μL or 82℃, 350 μL/125 μL) and heated for 30 min to dissolve D-OPE$_7$-*b*-PNIPAM$_{22}$, followed by adding 25 μL of L-OPE$_9$-*b*-P2VP$_{56}$ (L_n = 108 nm, 0.1 mg/mL in ethanol) seed micelles. After the resulting solutions were heated for another 10 s, they were cooled and aged at room temperature (23℃) for 24 h. TEM images are presented in **Figures 9B-D** & **S15**.

Preparation of ^{M}(S-OPE$_8$-*b*-PNIPAM$_{22}$)-*b*-^{M}(S-OPE$_9$-*b*-P2VP$_{56}$)-*b*-^{M}(S-OPE$_8$-*b*-PNIPAM$_{22}$) A-B-A triblock comicelles by seeded growth approach

Aliquots (1, 2, 3 and 4 μL) of a concentrated THF solution of S-OPE$_8$-*b*-PNIPAM$_{22}$ (2.5 mg/mL) were added into 475 μL of hot ethanol (70℃) and heated for 30 min to dissolve S-OPE$_8$-*b*-PNIPAM$_{22}$, followed by adding 25 μL of S-OPE$_9$-*b*-P2VP$_{56}$ (L_n = 108 nm, L_w/L_n = 1.11, 0.1 mg/mL in ethanol) seed micelles. After the resulting solutions were heated for another 10 s, they were cooled and aged at 23^{o}C for 24 h. The unimer-to-seed molar ratios were calculated to be about 1.8, 3.6, 5.4 and 7.2, respectively, for the addition of 1, 2, 3 and 4 μL of

THF solution of S-OPE$_8$-*b*-PNIPAM$_{22}$. TEM images are presented in Figures 9E-F & S16 and details are collected in **Table S7**.

Preparation of ^{M}(D-OPE$_8$-*b*-PNIPAM$_{22}$)-*b*-^{M}(S-OPE$_9$-*b*-P2VP$_{56}$)-*b*-^{M}(D-OPE$_8$-*b*-PNIPAM$_{22}$) A-B-A triblock comicelles by "heating/cooling" seeded growth approach

Aliquots (1, 2, 3 and 4 μL) of a concentrated THF solution of D-OPE$_8$-*b*-PNIPAM$_{22}$ (2.5 mg/mL) were added into 475 μL of hot ethanol (70°C) and heated for 30 min to dissolve S-OPE$_8$-*b*-PNIPAM$_{22}$, followed by adding 25 μL of S-OPE$_9$-*b*-P2VP$_{56}$ (L_n = 108 nm, 0.1 mg/mL in ethanol) seed micelles. After the resulting solutions were heated for another 10 s, they were cooled and aged at room temperature (23°C) for 24 h. The unimer-to-seed molar ratios were calculated to be about 1.7, 3.4, 5.1 and 6.8, respectively, for the addition of 1, 2, 3 and 4 μL of THF solution of D-OPE$_8$-*b*-PNIPAM$_{22}$. TEM images are presented in **Figures 9H-I** & **S17** and details are collected in **Table S8**.

ADDITIONAL RESULTS AND DISCUSSION

Since the calculated lengths of OPE_7 and OPE_8 segments (~5 nm) are comparable to the widths (~5-7 nm) of the formed fiber-like micelles, the OPE_7 and OPE_8 segments of these BCPs likely form the core of the micelles in a single layer face-to-face packing mode. We explain this result by assuming that the S-OPE_7, D-OPE_8, S-OPE_8 blocks of the BCPs minimize steric repulsion of the corona chains by stacking in a reverse face-to-face arrangement with certain degree of slippage to form J-aggregates as shown in **Scheme 2** (main text). Unlike the symmetric S-OPE_7, D-OPE_8, S-OPE_8 blocks, D-OPE_7 segments are asymmetric along the long axis. Some D-OPE_7 blocks of the BCPs also stacked face-to-face with certain slippages due to steric repulsion effect of PNIPAM corona chains as shown in Scheme 2. In addition, some D-OPE_7 blocks of the BCPs reversely stacked face-to-face without the slippage to form H-aggregates as shown in **Scheme 2**. X-ray diffraction measurements on S-OPE_8 and S-OPE_7 show two peaks at $2\theta = 6.6^o$ and 22.1^o, attributed to the ordered packing of hexyl side chains and π-π interaction of OPE units (**Figure S17**). Three peaks at $2\theta = 4.8^o$, 12.6^o and 23.4^o appeared in XRD pattern of D-OPE_8 (**Figure S17**). In contrast, five peaks with $2\theta = 4.1^o$, 6.1^o, 12.3^o, 18.8^o and 23.2^o were detected for D-OPE_7 (**Figure S17**). These observations further imply that D-OPE_7 units follow a different packing mode from those of S-OPE_7, S-OPE_8 and D-OPE_8.

SUPPORTING FIGURES

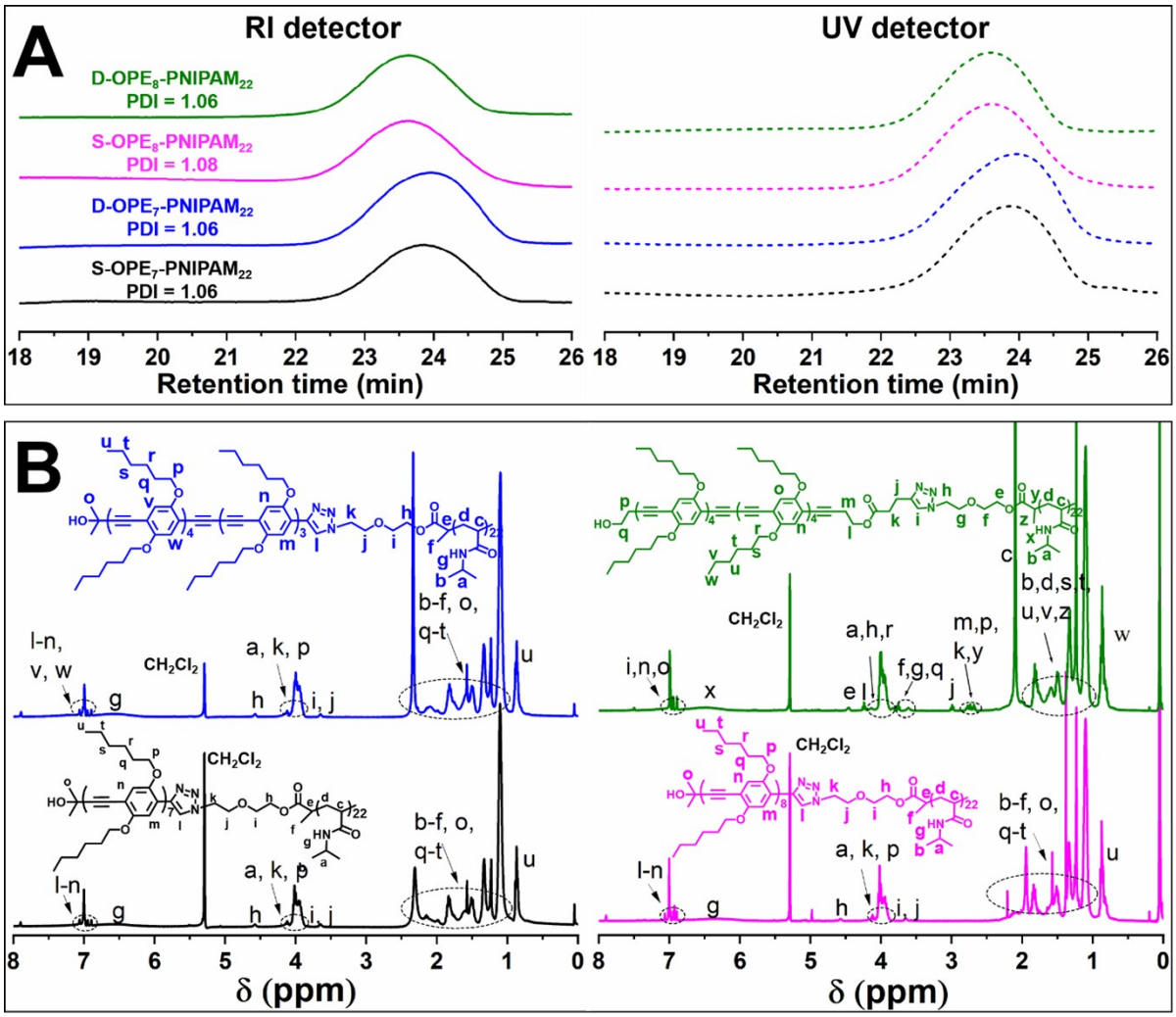

Figure S1. (A) SEC curves and (B) ^{1}H NMR spectra (in CD_2Cl_2) of S-OPE$_7$-*b*-PNIPAM$_{22}$, D-OPE$_7$-*b*-PNIPAM$_{22}$, S-OPE$_8$-*b*-PNIPAM$_{22}$ and D-OPE$_8$-*b*-PNIPAM$_{22}$.

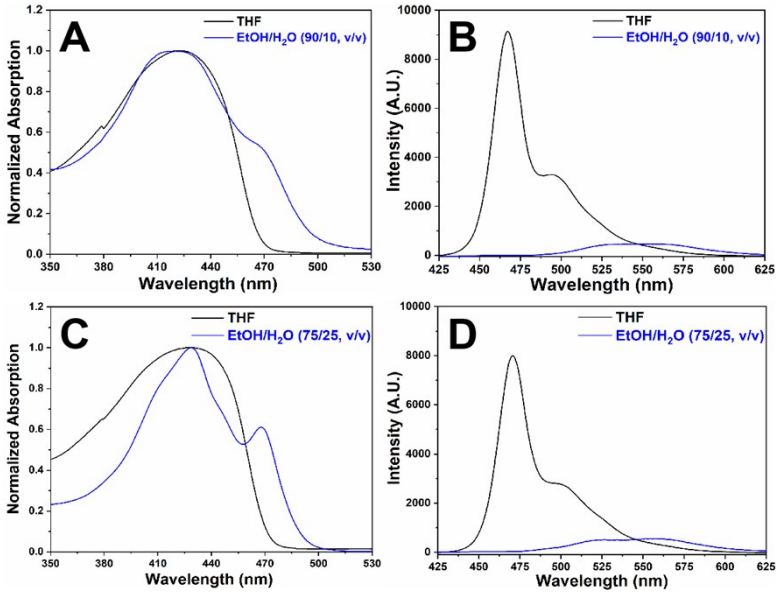

Figure S2. (A) UV/vis absorption and (B) fluorescent (λ_{ex} = 410 nm) spectra of S-OPE$_7$-*b*-PNIPAM$_{22}$ in THF (0.05 mg/mL) and ethanol/water (90/10, 0.05 mg/mL). (C) UV/vis absorption and (D) fluorescent (λ_{ex} = 410 nm) spectra of D-OPE$_7$-*b*-PNIPAM$_{22}$ in THF (0.05 mg/mL) and ethanol/water (75/25, v/v, 0.05 mg/mL).

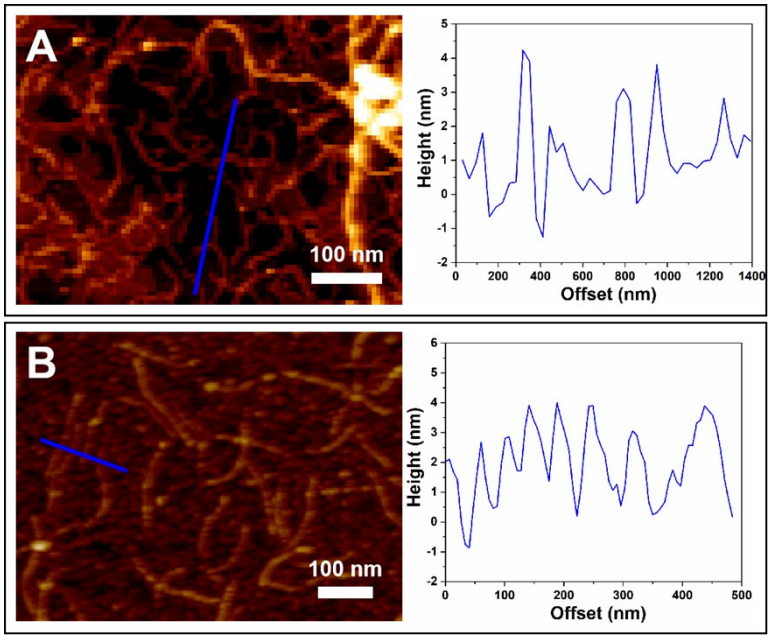

Figure S3. AFM images and corresponding height profiles of polydisperse micelles of (A) S-OPE$_7$-*b*-PNIPAM$_{22}$ in ethanol/water (90/10, v/v) and (B) D-OPE$_7$-*b*-PNIPAM$_{22}$ in ethanol/water (75/25, v/v) obtained by heating/cooling process as shown in Figure 2.

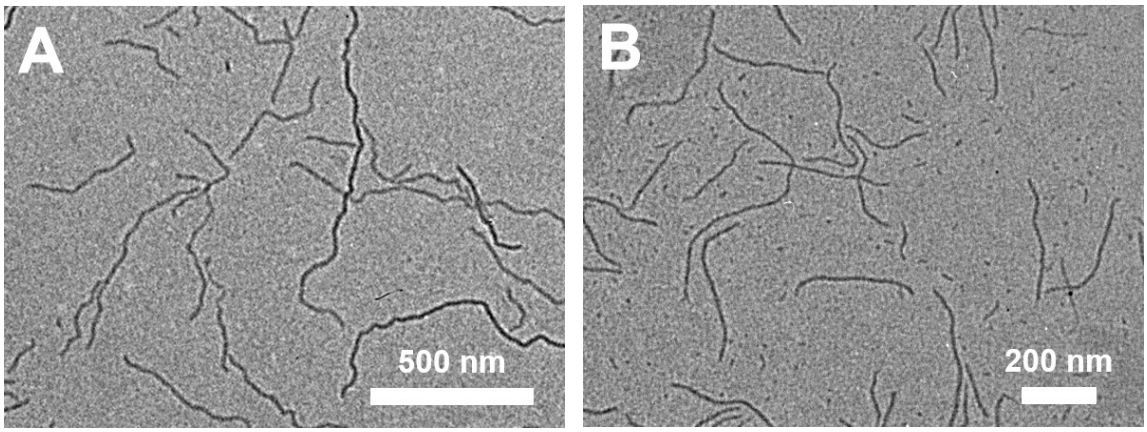

Figure S4. TEM images of micelles of (A) S-OPE$_7$-*b*-PNIPAM$_{22}$ in ethanol/water (90/10, v/v) and (B) D-OPE$_7$-*b*-PNIPAM$_{22}$ in ethanol/water (75/25, v/v) after aging at room temperature for 2 months.

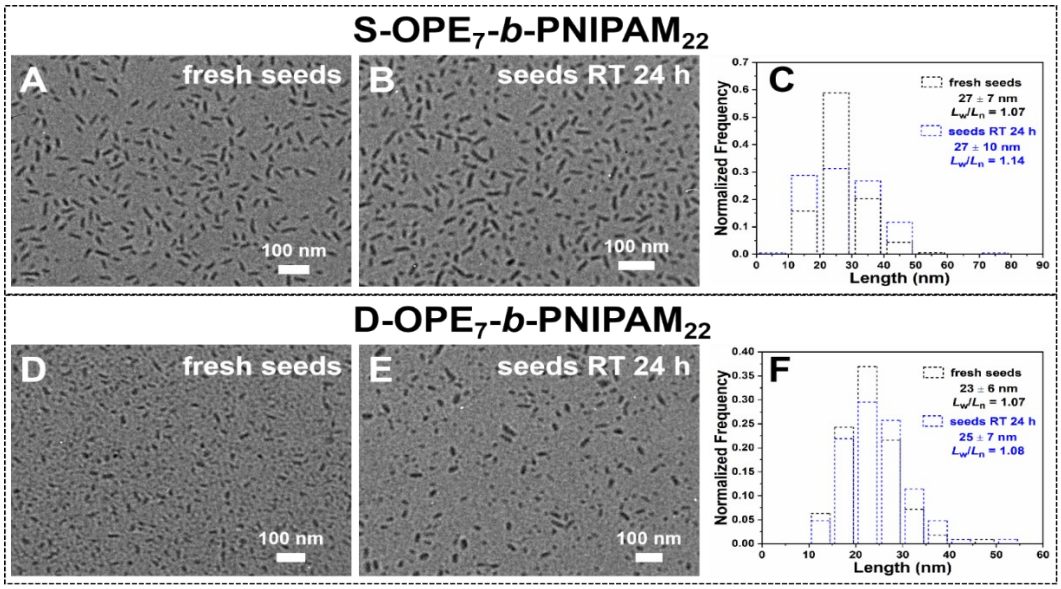

Figure S5. TEM images of (A) fresh seeds and (B) seeds of S-OPE$_7$-*b*-PNIPAM$_{22}$ in ethanol/water (90/10, v/v) after aging at room temperature for 24 h. (C) Length distributions of fresh seeds and seeds after aging at room temperature for 24 h micelles of S-OPE$_7$-*b*-PNIPAM$_{22}$. TEM images of (D) fresh seeds and (E) seeds of D-OPE$_7$-*b*-PNIPAM$_{22}$ in ethanol/water (75/25, v/v) after aging at room temperature for 24 h. (F) Length distributions of fresh seeds and seeds after aging at room temperature for 24 h micelles of D-OPE$_7$-*b*-PNIPAM$_{22}$.

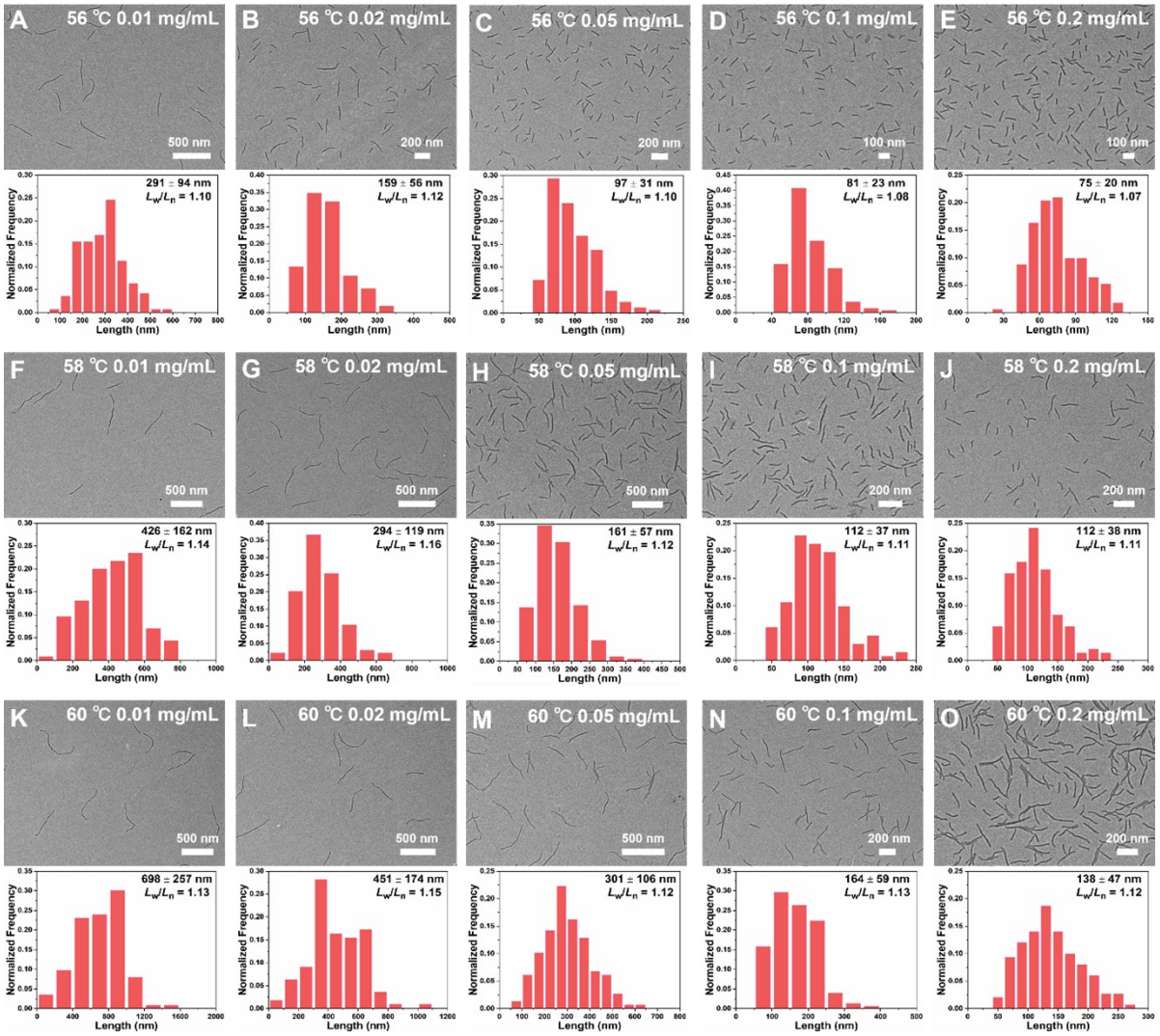

Figure S6. TEM images and length distribution of fiber-like micelles of S-OPE$_7$-*b*-PNIPAM$_{22}$ obtained by annealing the seeds at (A-E) 56℃, (F-J) 58℃ and (K-O) 60℃ in ethanol/water (90/10, v/v) with a concentration of (A, F, K) 0.01, (B, G, L) 0.02, (C, H, M) 0.05, (D, I, N) 0.1 and (E, J, O) 0.2 mg/mL and cooling/aging at room temperature.

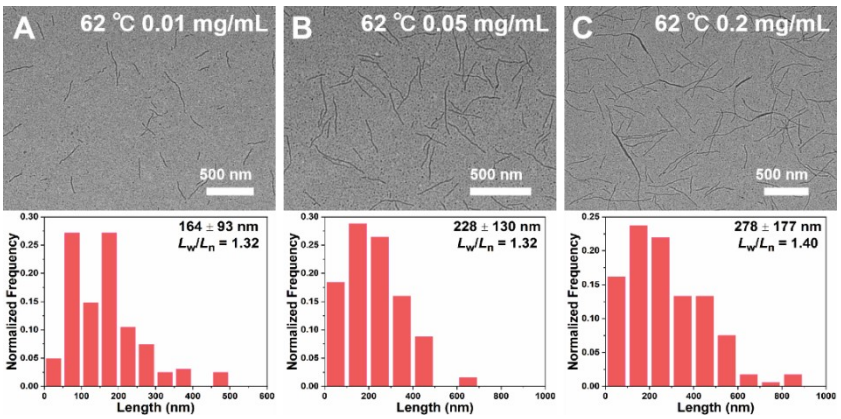

Figure S7. TEM images and length distribution of fiber-like micelles of D-OPE$_7$-*b*-PNIPAM$_{22}$ obtained by annealing the seeds at 62℃ in ethanol/water (90/10, v/v) with a concentration of (A) 0.01, (B) 0.05 and (C) 0.2 mg/mL and cooling/aging at room temperature.

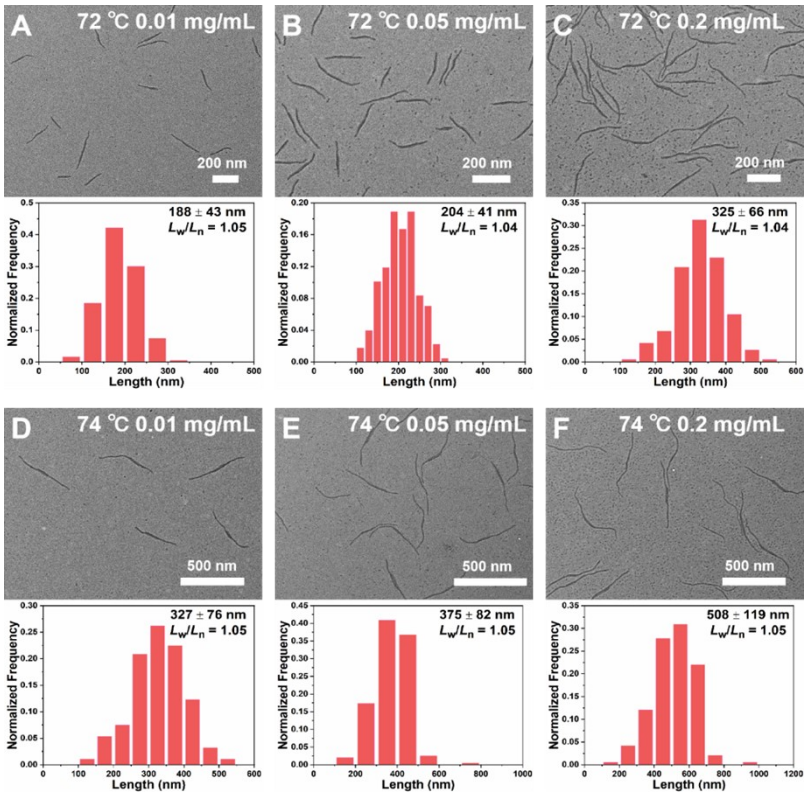

Figure S8. TEM images and length distribution of fiber-like micelles of D-OPE$_7$-*b*-PNIPAM$_{22}$ obtained by annealing the seeds at (A-C) 72℃ and (D-F) 74℃ in ethanol/water (75/25, v/v) with a concentration of (A & D) 0.01, (B & E) 0.05 and (C & F) 0.2 mg/mL and cooling/aging at room temperature.

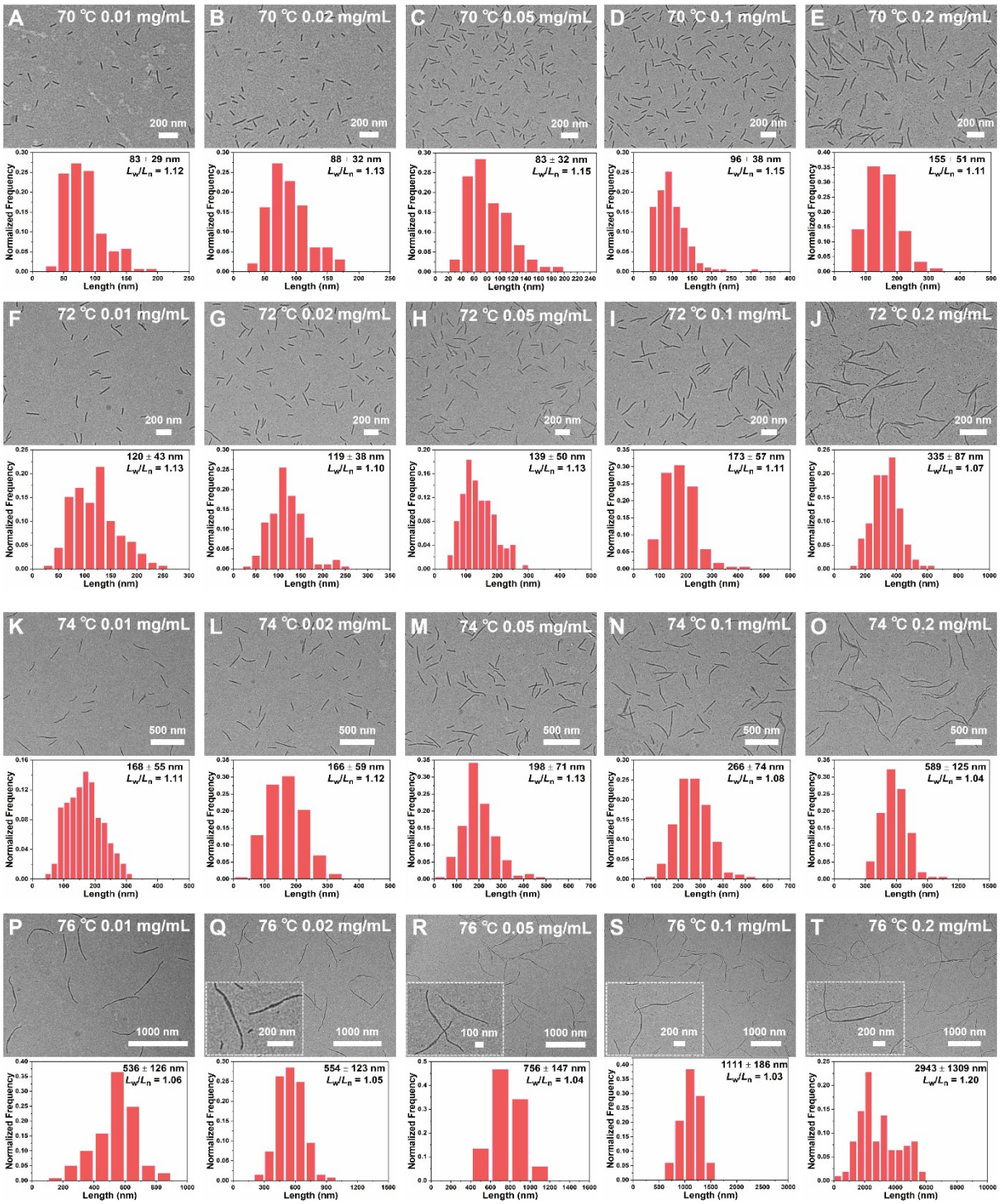

Figure S9. TEM images and length distribution of fiber-like micelles of D-OPE_7-*b*-$PNIPAM_{22}$ obtained by annealing the seeds at (A-E) 70°C, (F-J) 72°C, (K-O) 74°C and (P-T) 76°C in ethanol/water (75/25, v/v) with a concentration of (A, F, K, P) 0.01, (B, G, L, Q) 0.02, (C, H, M, R) 0.05, (D, I, N, S) 0.1 and (E, J, O, T) 0.2 mg/mL and cooling/aging with water-bath.

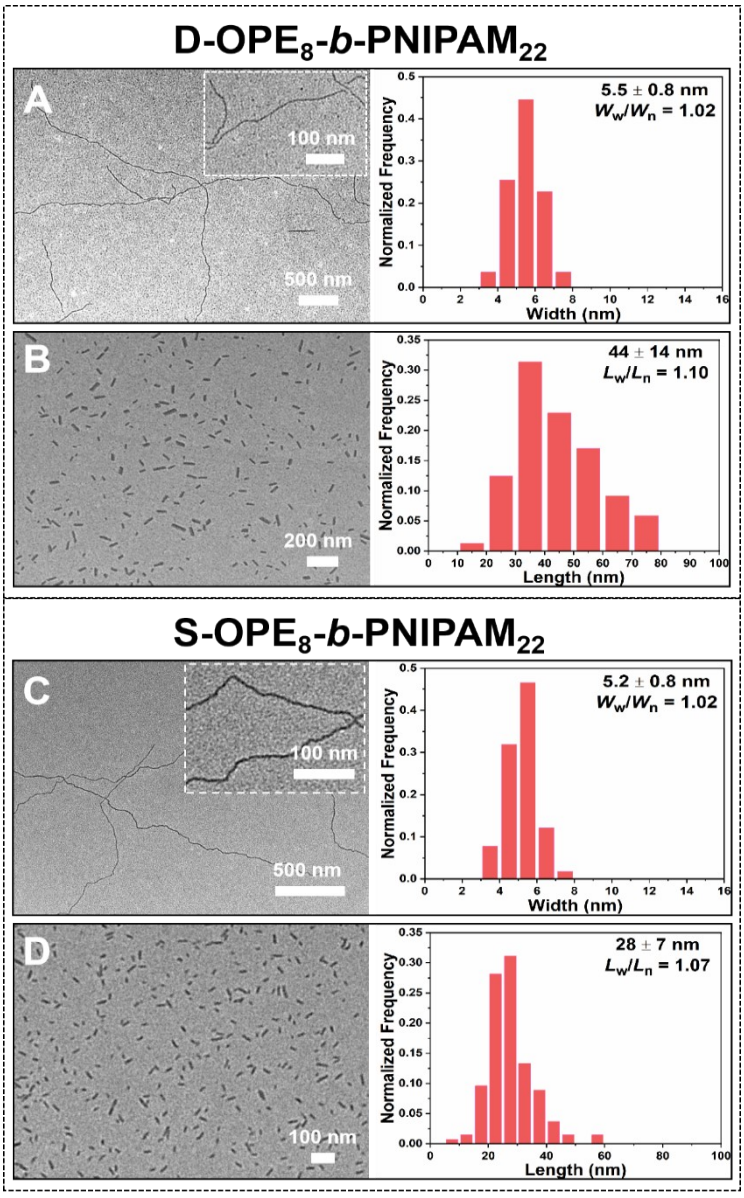

Figure S10. (A) TEM image and width distribution histograms of polydisperse fiber-like micelles of D-OPE$_8$-*b*-PNIPAM$_{22}$ obtained by heating/cooling process in ethanol. (B) TEM image and length distribution histograms of seed micelles of D-OPE$_8$-*b*-PNIPAM$_{22}$ obtained by sonication of as-prepared polydisperse fiber-like micelles. (C) TEM image and width distribution histograms of polydisperse fiber-like micelles of S-OPE$_8$-*b*-PNIPAM$_{22}$ obtained by heating/cooling process in ethanol. (D) TEM image and length distribution histograms of seed micelles of S-OPE$_8$-*b*-PNIPAM$_{22}$ obtained by sonication of as-prepared polydisperse fiber-like micelles.

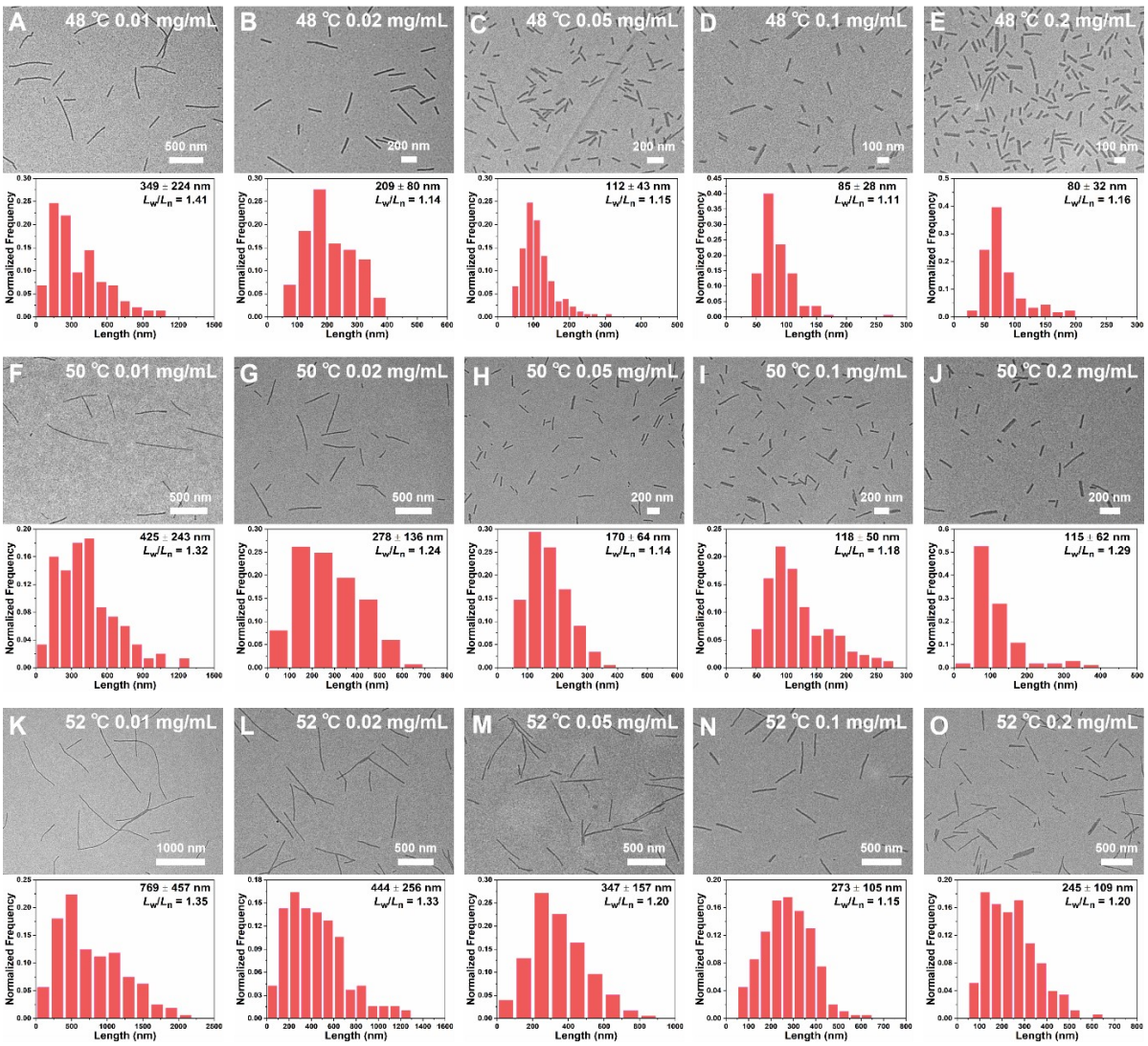

Figure S11. TEM images and length distribution of ribbon/fiber-like micelles of D-OPE_8-*b*-$PNIPAM_{22}$ obtained by annealing the seeds at (A-E) 48℃, (F-J) 50℃ and (K-O) 52℃ in ethanol with concentration of (A, F, K) 0.01, (B, G, L) 0.02, (C, H, M) 0.05, (D, I, N) 0.1 and (E, J, O) 0.2 mg/mL and cooling/aging by immersing the vials into water 35℃.

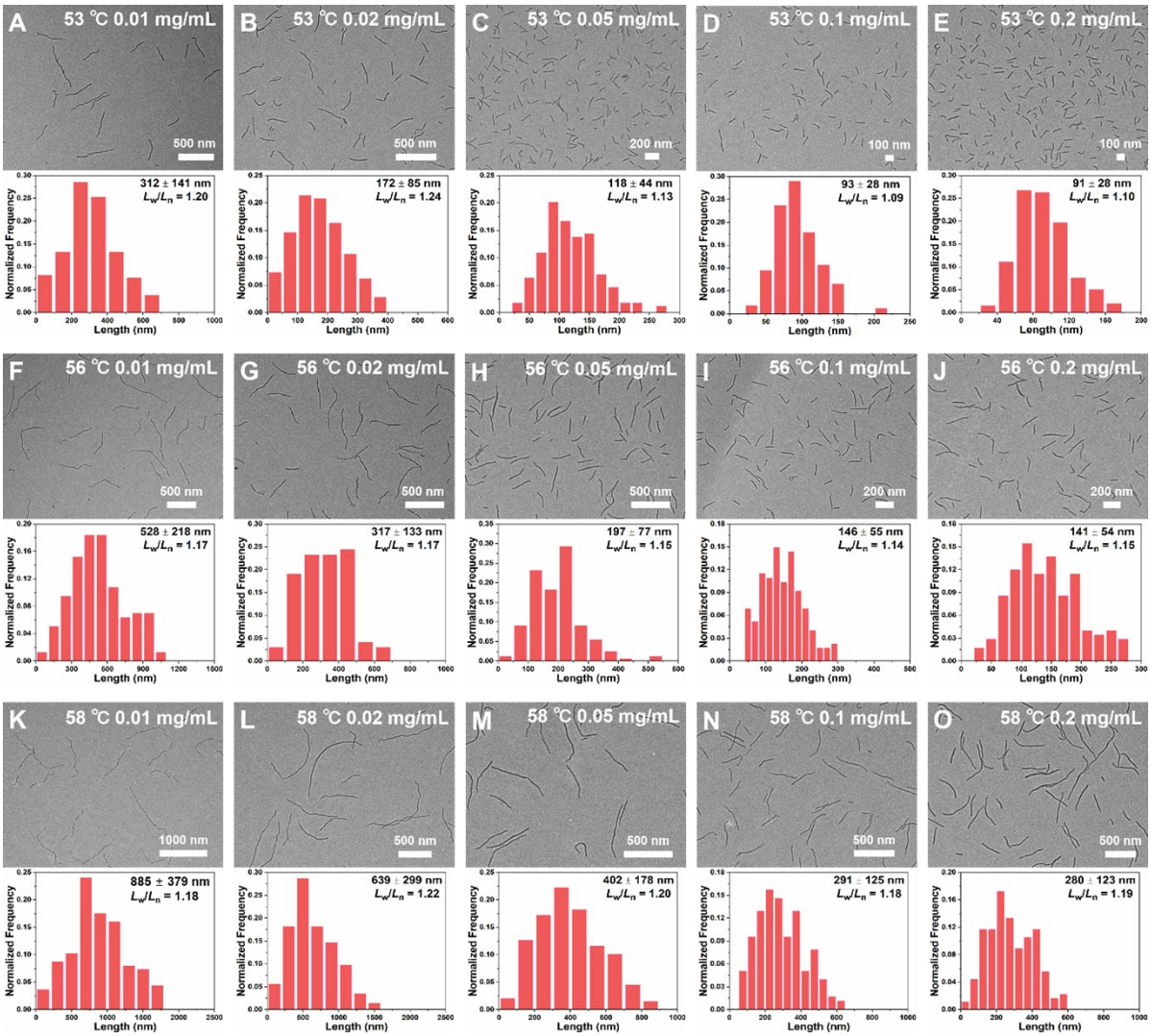

Figure S12. TEM images and length distribution of fiber-like micelles of S-OPE$_8$-*b*-PNIPAM$_{22}$ obtained by annealing the seeds at (A-E) 53℃, (F-J) 56℃ and (K-O) 58℃ in ethanol with a concentration of (A, F, K) 0.01, (B, G, L) 0.02, (C, H, M) 0.05, (D, I, N) 0.1 and (E, J, O) 0.2 mg/mL and cooling/aging at room temperature.

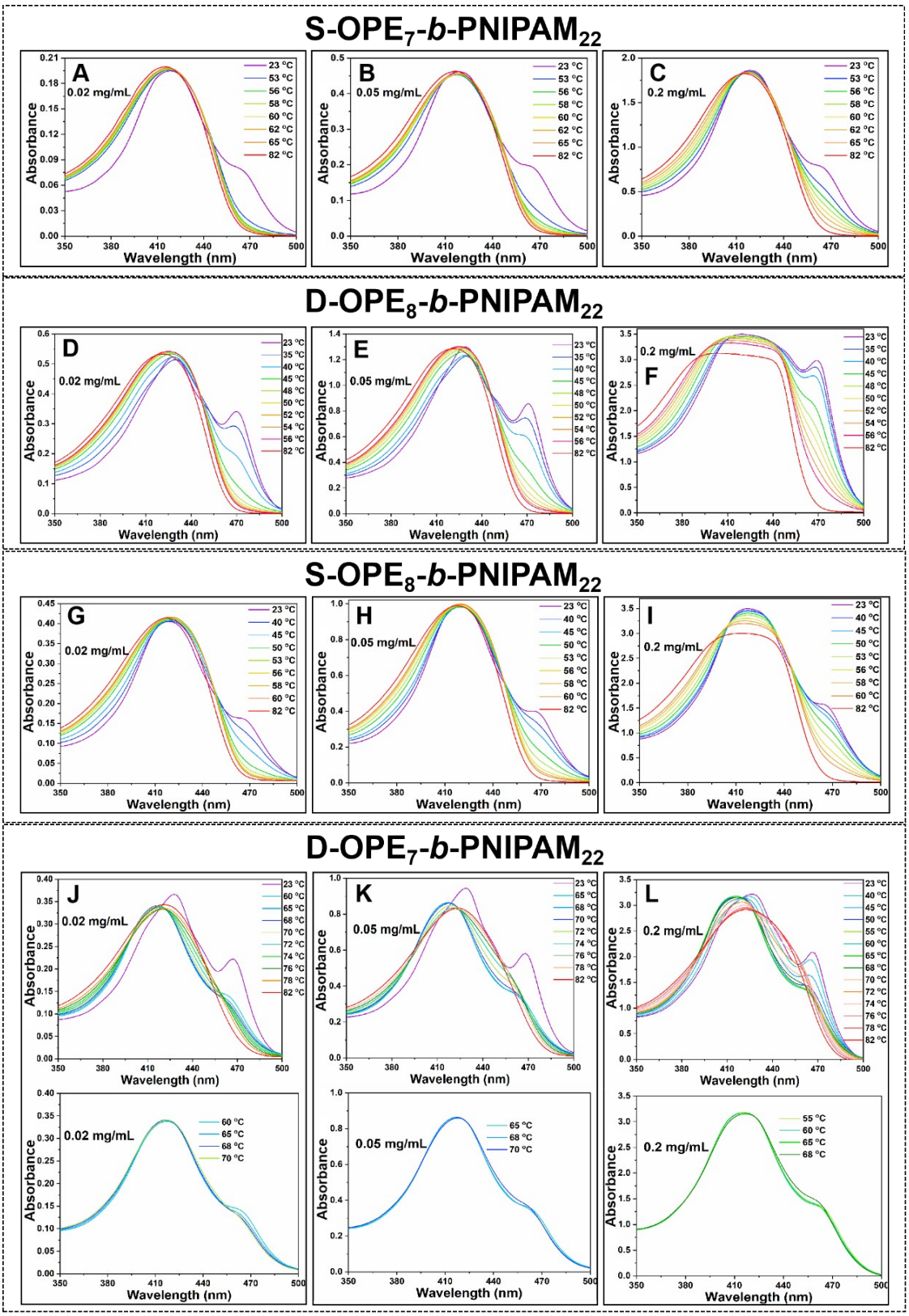

Figure S13. Temperature-dependent UV/vis absorption spectra of seed micelles of (A-C) S-OPE_7-*b*-$PNIPAM_{22}$, (D-F) D-OPE_8-*b*-$PNIPAM_{22}$, (G-J) S-OPE_8-*b*-$PNIPAM_{22}$ and (K-M) D-OPE_7-*b*-$PNIPAM_{22}$ with different concentrations of 0.02, 0.05 and 0.2 mg/mL.

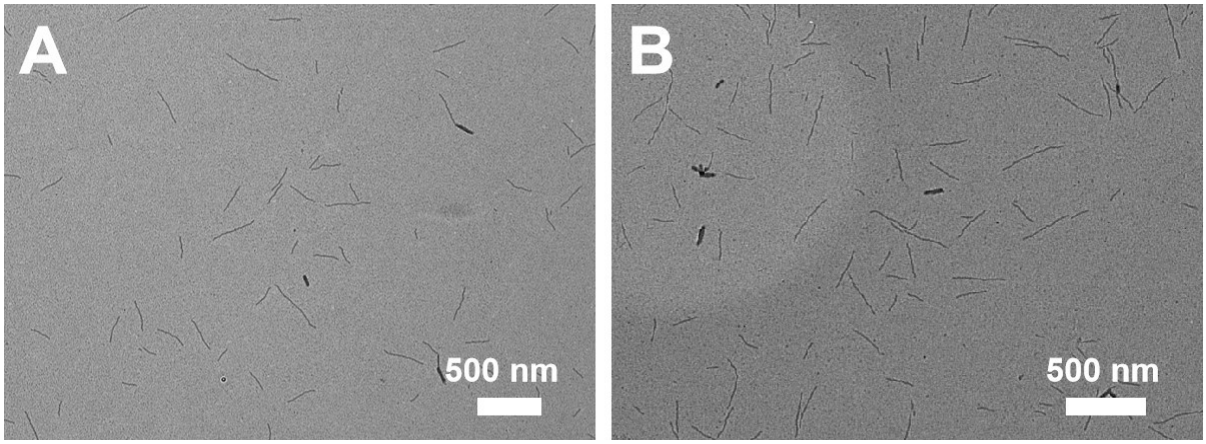

Figure S14 TEM images of co-micelles formed by adding 25 μL of S-OPE$_9$-*b*-P2VP$_{56}$ seeds in ethanol (0.1 mg/mL) to 475 μL of ethanol/water (415 μL/60 μL) solution of D-OPE$_7$-*b*-PNIPAM$_{22}$ at 70℃, followed by cooling/aging at room temperature (23℃) with n_{unimer}/n_{seed} of (A) 1.9 and (B) 5.7.

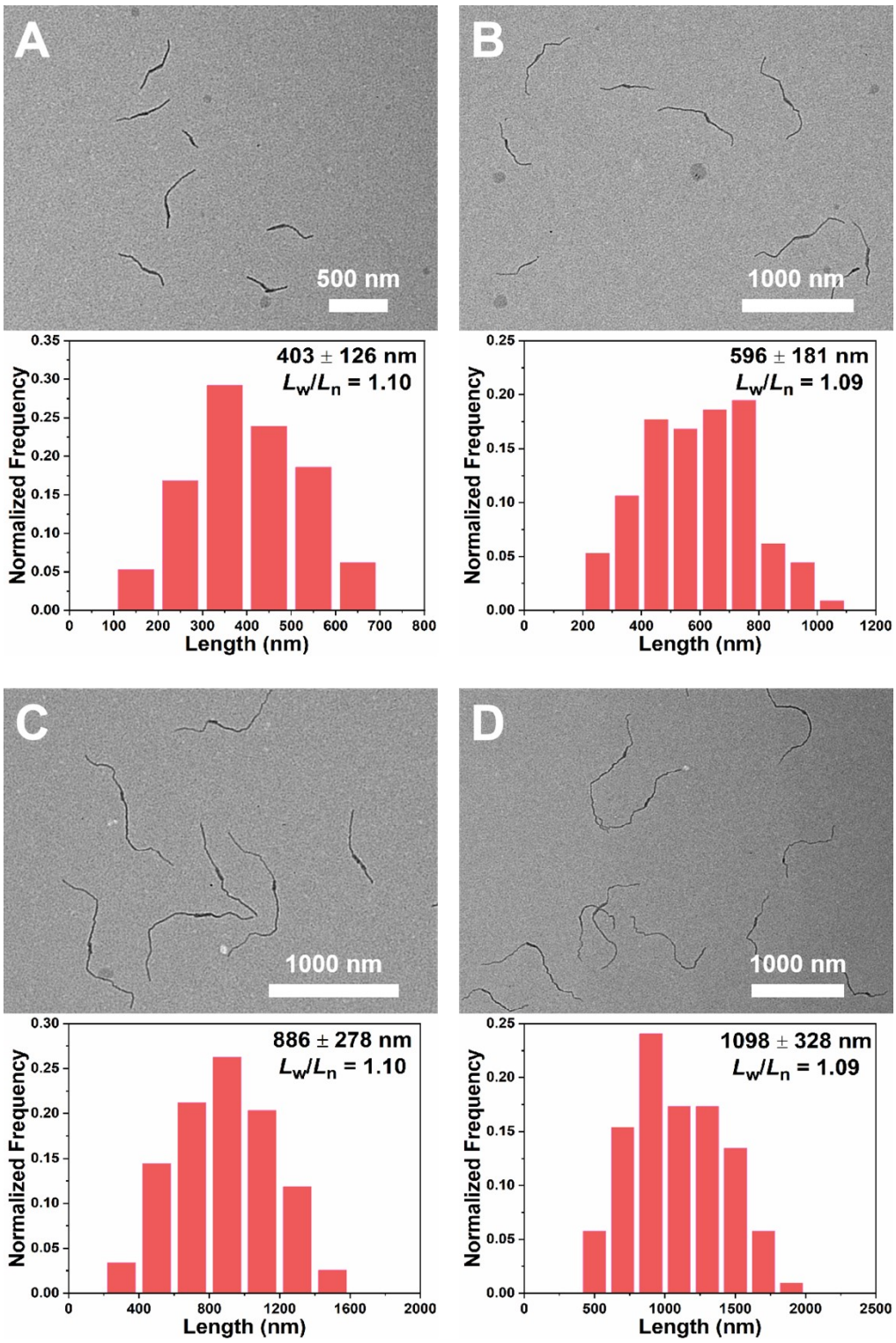

Figure S15 TEM images and length distribution of triblock co-micelles formed by adding 25 μL of S-OPE$_9$-*b*-P2VP$_{56}$ seeds in ethanol (0.1 mg/mL) to 475 μL of ethanol solution of S-OPE$_8$-*b*-PNIPAM$_{22}$ at 70°C with n_{unimer}/n_{seed} of (A) 1.8, (B) 3.6, (C) 5.4 and (D) 7.2, followed by cooling/aging at room temperature.

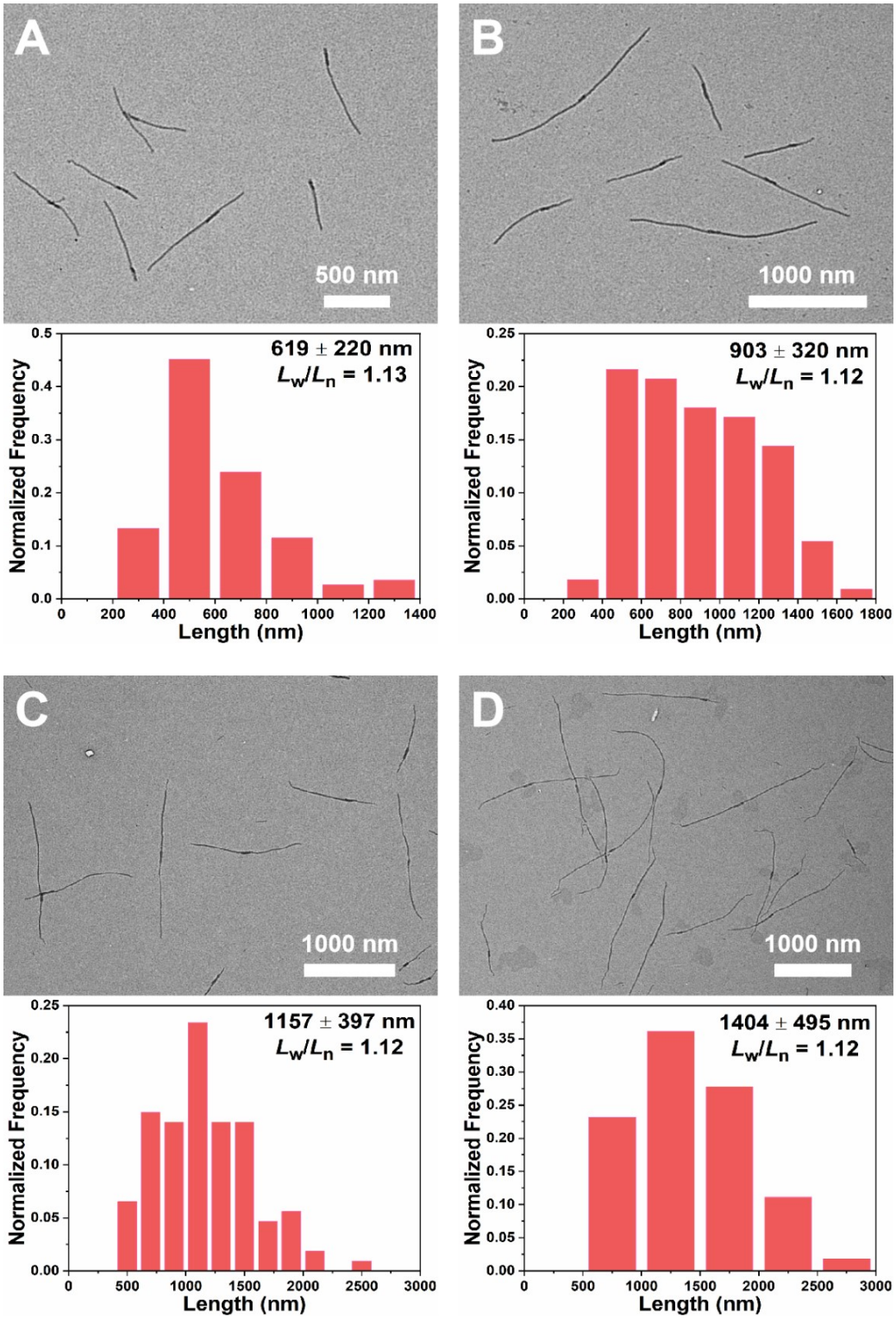

Figure S16 TEM images and length distribution of triblock co-micelles formed by adding 25 μL of S-OPE$_9$-*b*-P2VP$_{56}$ seeds in ethanol (0.1 mg/mL) to 475 μL of ethanol solution of D-OPE$_8$-*b*-PNIPAM$_{22}$ at 70°C with n_{unimer}/n_{seed} of (A) 1.7, (B) 3.4, (C) 5.1 and (D) 6.8, followed by cooling/aging at room temperature.

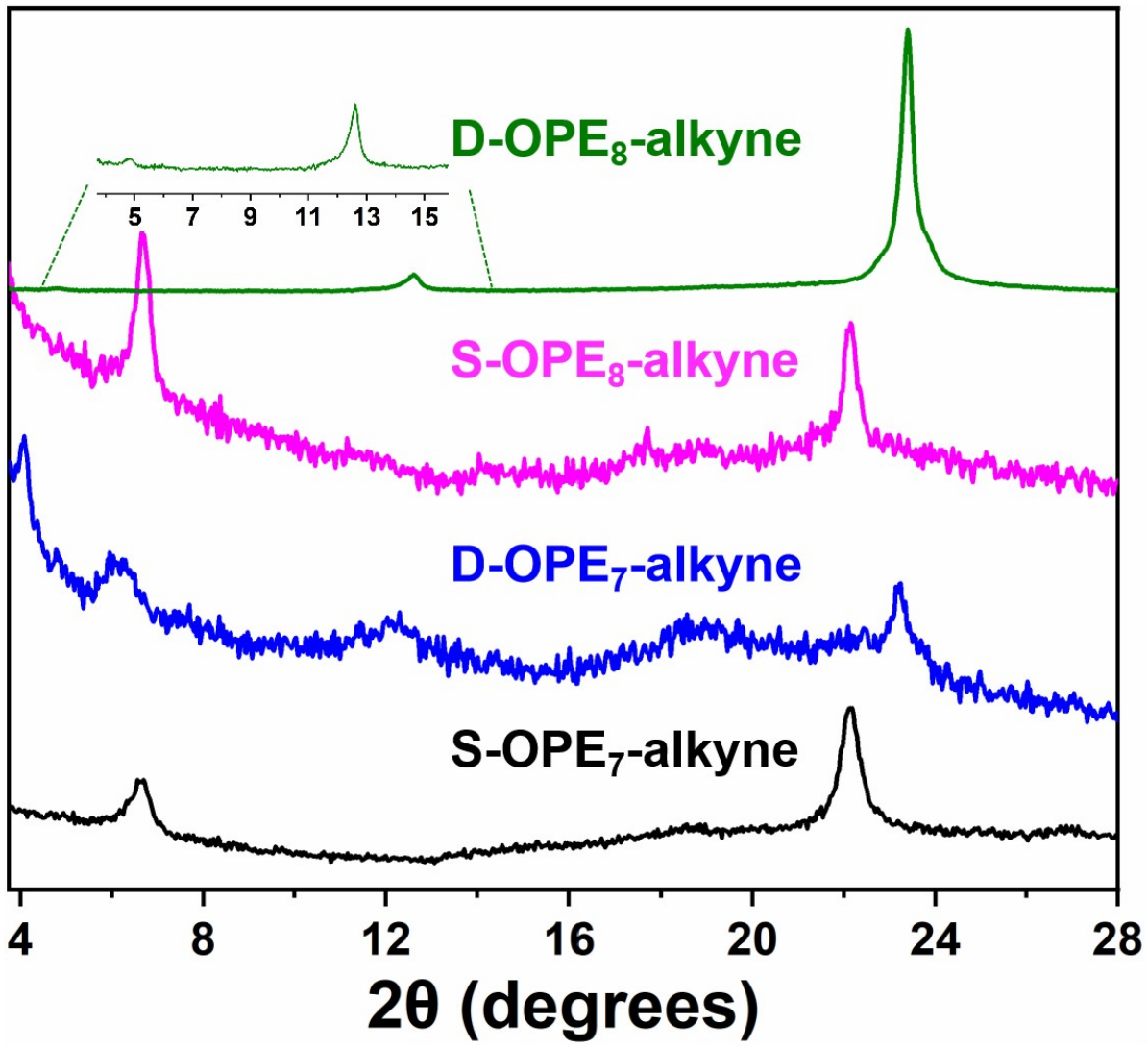

Figure S17. XRD patterns of S-OPE$_7$-alkyne, D-OPE$_7$-alkyne, S-OPE$_8$-alkyne and D-OPE$_8$-alkyne.

SUPPORTING TABLES

Table S1. Characteristics of seed micelles and elongated micelles of S-OPE$_7$-*b*-PNIPAM$_{22}$ obtained by annealing the seeds in ethanol/water (90/10, v/v) at different temperature and concentration then cooling/aging at room temperature[a]

T (°C)-*c* (mg/mL)	L_n (nm)	L_w (nm)	L_w/L_n[b]	σ[b] (nm)	σ/L_n[b]
seed	27	28	1.07	7	0.26
56-0.01	291	321	1.10	94	0.32
56-0.02	159	178	1.12	56	0.35
56-0.05	97	107	1.10	31	0.32
56-0.1	81	87	1.08	23	0.28
56-0.2	75	80	1.07	20	0.27
58-0.01	426	487	1.14	162	0.38
58-0.02	294	342	1.16	119	0.40
58-0.05	161	181	1.12	57	0.35
58-0.1	112	124	1.11	37	0.33
58-0.2	112	124	1.11	38	0.34
60-0.01	698	792	1.13	257	0.37
60-0.02	451	518	1.15	174	0.39
60-0.05	301	338	1.12	106	0.35
60-0.1	164	185	1.13	59	0.36
60-0.2	138	155	1.12	47	0.34

[a] The mean length of micelles was calculated from measurements of over 100 individual micelles in multiple TEM images.

[b] L_n, L_w and σ are number-average micelle length, weight-average micelle length and standard deviation of micelle length distribution, respectively, as calculated from the histogram of length distribution.

Table S2. Characteristics of elongated micelles of D-OPE$_7$-*b*-PNIPAM$_{22}$ obtained by annealing the seeds in ethanol/water (90/10, v/v) at different concentration then cooling/aging at room temperature [a]

T (°C)-*c* (mg/mL)	L_n (nm)	L_w (nm)	L_w/L_n[b]	σ[b] (nm)	σ/L_n[b]
62-0.01	164	217	1.32	93	0.57
62-0.05	228	301	1.32	130	0.57
62-0.2	278	390	1.40	177	0.64

[a] The mean length of micelles was calculated from measurements of over 100 individual micelles in multiple TEM images. The short stubby micelles with L_n below 20 nm that were formed at concentration of 0.1 and 0.2 mg/mL due to self-nucleation (Figure S9) were not measured and counted. If the contribution from short stubby micelles were counted, the value of length distribution would increase obviously.

[b] L_n, L_w and σ are number-average micelle length, weight-average micelle length and standard deviation of micelle length distribution, respectively, as calculated from the histogram of length distribution.

Table S3. Characteristics of elongated micelles of D-OPE$_7$-*b*-PNIPAM$_{22}$ obtained by annealing the seeds in ethanol/water (75/25, v/v) at different temperature and concentration then cooling/aging at room temperature [a]

T (^{o}C)-*c* (mg/mL)	L_n (nm)	L_w (nm)	L_w/L_n[b]	σ[b] (nm)	σ/L_n[b]
72 0.01	188	198	1.05	43	0.23
72 0.05	204	212	1.04	41	0.20
72 0.2	325	338	1.04	66	0.20
74 0.01	327	345	1.05	76	0.23
74 0.05	375	392	1.05	82	0.22
74 0.2	508	535	1.05	119	0.23

[a] The mean length of micelles was calculated from measurements of over 100 individual micelles in multiple TEM images. The short stubby micelles with L_n below 20 nm that were formed at concentration of 0.1 and 0.2 mg/mL due to self-nucleation (Figure S9) were not measured and counted. If the contribution from short stubby micelles were counted, the value of length distribution would increase obviously.

[b] L_n, L_w and σ are number-average micelle length, weight-average micelle length and standard deviation of micelle length distribution, respectively, as calculated from the histogram of length distribution.

Table S4. Characteristics of seed micelles and elongated micelles of D-OPE_7-*b*-$PNIPAM_{22}$ obtained by annealing the seeds in ethanol/water (75/25, v/v) at different temperature and concentration then cooling/aging with water-bath[a]

T (°C)-*c* (mg/mL)	L_n (nm)	L_w (nm)	L_w/L_n[b]	σ[b] (nm)	σ/L_n[b]
seed	23	25	1.07	6	0.26
70-0.01	83	93	1.12	29	0.35
70-0.02	83	95	1.15	32	0.39
70-0.05	88	100	1.13	32	0.36
70-0.1	96	111	1.15	38	0.39
70-0.2	155	172	1.11	51	0.33
72-0.01	120	136	1.13	43	0.36
72-0.02	119	131	1.10	38	0.32
72-0.05	139	157	1.13	50	0.36
72-0.1	173	191	1.11	57	0.33
72-0.2	335	357	1.07	87	0.26
74-0.01	168	186	1.11	55	0.33
74-0.02	166	186	1.12	59	0.35
74-0.05	198	223	1.13	71	0.36
74-0.1	266	286	1.08	74	0.28
74-0.2	589	615	1.04	125	0.21
76-0.01	536	566	1.06	126	0.24
76-0.02	554	581	1.05	123	0.22
76-0.05	756	784	1.04	147	0.19
76-0.1	1111	1142	1.03	186	0.17
76-0.2	2943	3519	1.20	1309	0.44

[a] The mean length of micelles was calculated from measurements of over 100 individual micelles in multiple TEM images. The short stubby micelles with L_n below 20 nm that were formed at concentration of 0.1 and 0.2 mg/mL due to self-nucleation (Figure S9) were not

measured and counted. If the contribution from short stubby micelles were counted, the value of length distribution would increase obviously.

[b] L_n, L_w and σ are number-average micelle length, weight-average micelle length and standard deviation of micelle length distribution, respectively, as calculated from the histogram of length distribution.

Table S5. Characteristics of seed micelles and elongated micelles of D-OPE_8-*b*-$PNIPAM_{22}$ obtained by annealing the seeds in ethanol at different temperature and concentration then cooling/aging by immersing the vials into water with temperature of 35 °C. [a]

T (°C)-*c* (mg/mL)	L_n (nm)	L_w (nm)	L_w/L_n[b]	σ[b] (nm)	$σ/L_n$[b]
seed	44	48	1.10	14	0.31
48-0.01	349	492	1.41	224	0.64
48-0.02	209	240	1.14	80	0.38
48-0.05	112	129	1.15	43	0.39
48-0.1	85	94	1.11	28	0.34
48-0.2	80	93	1.16	32	0.40
50-0.01	425	563	1.32	243	0.57
50-0.02	278	344	1.24	136	0.49
50-0.05	170	194	1.14	64	0.38
50-0.1	118	139	1.18	50	0.42
50-0.2	115	149	1.29	62	0.54
52-0.01	769	1039	1.35	457	0.59
52-0.02	444	591	1.33	256	0.58
52-0.05	347	418	1.20	157	0.45
52-0.1	273	313	1.15	105	0.38
52-0.2	245	293	1.20	109	0.44

[a] The mean length of micelles was calculated from measurements of over 100 individual micelles in multiple TEM images.

[b] L_n, L_w and σ are number-average micelle length, weight-average micelle length and standard deviation of micelle length distribution, respectively, as calculated from the histogram of length distribution.

Table S6. Characteristics of seed micelles and elongated micelles of S-OPE$_8$-*b*-PNIPAM$_{22}$ obtained by annealing the seeds in ethanol at different temperature and concentration then cooling/aging at room temperature[a]

T (^{o}C)-*c* (mg/mL)	L_n (nm)	L_w (nm)	L_w/L_n[b]	σ[b] (nm)	σ/L_n[b]
seed	28	30	1.07	7	0.26
53-0.01	312	376	1.20	141	0.45
53-0.02	172	214	1.24	85	0.49
53-0.05	118	134	1.13	44	0.37
53-0.1	93	102	1.09	28	0.31
53-0.2	91	100	1.10	28	0.31
56-0.01	528	618	1.17	218	0.41
56-0.02	317	373	1.17	133	0.42
56-0.05	197	227	1.15	77	0.39
56-0.1	146	166	1.14	55	0.38
56-0.2	141	162	1.15	54	0.38
58-0.01	885	1046	1.18	379	0.43
58-0.02	639	778	1.22	299	0.47
58-0.05	402	481	1.20	178	0.44
58-0.1	291	345	1.18	125	0.43
58-0.2	280	333	1.19	123	0.44

[a] The mean length of micelles was calculated from measurements of over 100 individual micelles in multiple TEM images.

[b] L_n, L_w and σ are number-average micelle length, weight-average micelle length and standard deviation of micelle length distribution, respectively, as calculated from the histogram of length distribution.

Table S7. Characteristics of seed micelles of S-OPE$_9$-*b*-P2VP$_{56}$ and elongated fiber-like of ^{M}(S-OPE$_8$-*b*-PNIPAM$_{22}$)-*b*-^{M}(S-OPE$_9$-*b*-P2VP$_{56}$)-*b*-^{M}(S-OPE$_8$-*b*-PNIPAM$_{22}$) A-B-A triblock comicelles obtained by heating/cooling seeded growth approach[a]

V (μL)	n_{unimer}/n_{seed}	L_n (nm)	L_w (nm)	L_w/L_n[b]	σ[b] (nm)	$σ/L_n$[b]
0	seed	118	137	1.16	47	0.40
1	1.8	403	442	1.10	126	0.31
2	3.6	596	650	1.09	181	0.30
3	5.4	886	972	1.10	278	0.31
4	7.2	1098	1195	1.09	328	0.30

[a] The mean length of micelles was calculated from measurements of over 100 individual micelles in multiple TEM images.

[b] L_n, L_w and σ are number-average micelle length, weight-average micelle length and standard deviation of micelle length distribution, respectively, as calculated from the histogram of length distribution.

Table S8. Characteristics of seed micelles of S-OPE$_9$-*b*-P2VP$_{56}$ and elongated fiber-like of ^{M}(D-OPE$_8$-*b*-PNIPAM$_{22}$)-*b*-^{M}(S-OPE$_9$-*b*-P2VP$_{56}$)-*b*-^{M}(D-OPE$_8$-*b*-PNIPAM$_{22}$) A-B-A triblock comicelles obtained by heating/cooling seeded growth approach[a]

V (μL)	n_{unimer}/n_{seed}	L_n (nm)	L_w (nm)	L_w/L_n[b]	σ[b] (nm)	$σ/L_n$[b]
0	seed	118	137	1.16	47	0.40
1	1.7	619	697	1.13	220	0.36
2	3.4	903	1016	1.12	320	0.35
3	5.1	1157	1292	1.12	397	0.34
4	6.8	1404	1577	1.12	495	0.35

[a] The mean length of micelles was calculated from measurements of over 100 individual micelles in multiple TEM images.

[b] L_n, L_w and σ are number-average micelle length, weight-average micelle length and standard deviation of micelle length distribution, respectively, as calculated from the histogram of length distribution.

References and Notes

1. Nie, J. C.; Wang, Z. Q.; Huang, X. Y.; Lu, G. L.; Feng, C. Uniform continuous and segmented nanofibers containing a π-conjugated oligo(*p*-phenylene ethynylene) core via "living" crystallization-driven self-assembly: Importance of oligo(*p*-phenylene ethynylene) chain length. *Macromolecules* **2020**, *53*, 6299-6313.